Developmental reprogramming of splenic vasculature and homeostasis of B-1a cells in Nkx2.3 homeodomain transcription factor deficient mouse model

PhD thesis

Dr. Árpád Lábadi

PTE, Department of Immunology and Biotechnology

Supervisor: Dr. Péter Balogh

2014.

Table of Content

List of abbreviations

AFC	antibody forming cells
AGM	aorto-gonad mesonephros
BCR	B-cell receptor
CFSE	carboxyfluorescein diacetate succinimidyl ester
DC	dendritic cell
DMSO	dimethyl sulfoxide
ENU	n-ethyl-n-nitrosourea
FDC	follicular dendritic cells
Fo	follicle
FSC	forward scatter
GC	germinal center
HD	homeodomain
HEV	high endothelial venule
hi	high
i.p.	intraperitoneally
i.v.	intravenous / intravenously
Id2	Inhibitor of DNA binding 2
Ig	immunoglobulin
IgA	immunoglobulin A isotype
IgD	immunoglobulin D isotype
IgG	immunoglobulin G isotype
IgL	immunoglobulin light chain
IgM	immunoglobulin M isotype
IL	interleukin
ILC	innate lymphoid cell
ILF	isolated lymphoid follicles
ILL	innate-like lymphocyte
LEC	lymphatic endothelium cell
LN	lymph node
lo	low
LTi	lymphoid tissue inducer

LTα	lymphotoxin alpha
LTβ	lymphotoxin beta
LTβR	lymphotoxin beta receptor
mAb	monoclonal antibody
MAdCAM-1	Mucosal Addressin Cell Adhesion Molecule 1
MARCO	macrophage receptor with collagenous structure
mLN	mesenteric lymph node
MS	marginal sinus
MZ	marginal zone
MzB cells	marginal zone B lymphocytes
NK	natural killer
NKT	natural killer T
PALS	peri-arteriolar lymphatic sheath
PAS	para-aortic splanchnopleura
Pc	phosphorylcholine
pLN	peripheral lymph node
PNAd	peripheral node addressin
PPS	pneumococcus polysaccharide
RORγt	retinoic acid-related orphan receptor γ t
RP	red pulp
SEM	standard error of the mean
SIGLEC1	sialic-acid-binding immunoglobulin-like lectin 1
spl	spleen
SSC	side scatter
TCR	T-cell receptor
T_{FH}	follicular T helper cells
VEGFR	vascular endothelial growth factor receptor
wt	wild-type

Publications the thesis is based on

First authorship

Lábadi A, Balogh P. Differential preferences in serosal homing and distribution of peritoneal B-cell subsets revealed by in situ CFSE labeling. *Int. Immunol.* 2009; **21**:1047–56.DOI: 10.1093/intimm/dxp071.

IF: 3,403

Second authorship

Czömpöly T**, Lábadi A,** Kellermayer Z, Olasz K, Arnold H-H, Balogh P. Transcription factor Nkx2.3 controls the vascular identity and lymphocyte homing in the spleen. *J. Immunol.* 2011; **186**:6981–9.DOI: 10.4049/jimmunol.1003770.

IF: 5,788 (from this 2,894 is used for this dissertation)

Publications not directly related to this essay

Shared first authorship

Kellermayer Z**, Lábadi A,** Czömpöly T, Arnold H-H, Balogh P. Absence of Nkx2.3 homeodomain transcription factor induces the formation of LYVE-1-positive endothelial cysts without lymphatic commitment in the spleen. *J. Histochem. Cytochem.* 2011; **59**:690–700.DOI: 10.1369/0022155411410061.

IF: 2,725

Second authorship

Czömpöly T, **Lábadi A,** Balázs M, Németh P, Balogh P. Use of cyclic peptide phage display library for the identification of a CD45RC epitope expressed on murine B cells and their precursors. *Biochem. Biophys. Res. Commun.* 2003; **307**:791–6.

IF: 2,836

Total IF: 14.752

Book chapter:

Developmental Biology of Peripheral Lymphoid Organs, 2011 Springer
Editor: Dr. Péter Balogh
Chapter 11.: Structural Evolution of the Spleen in Man and Mouse
Péter Balogh and Árpád Lábadi

Conferences:

May, 2008. ISAC XXIV International Congress, Budapest. *Defects of peritoneal B-1 B-cell homeostasis in the absence of Nkx2.3 homeodomain transcription factor*
(Poster presentation)

October, 2008. XXXVII. Annual Meeting of the Hungarian Society of Immunology. "Peritoneális B-1 B sejtek homeosztázisának defektusa Nkx2.3 homeodomén transzkripciós faktor hiányában"
(Oral presentation)

July, 2009. 16th Germinal Center Conference, Frankfurt, Germany. *Immunological Competence of the spleen is determined through its prenatal vascular commitment involving homeodomain factor Nkx2.3*
(Poster presentation)

September, 2009. 2nd European Congress of Immunology, Berlin, Germany. *Defects of peritoneal B-1 B-cell homeostasis in the absence of Nkx2.3 homeodomain transcription factor* (Oral presentation)

November 2010. 7th International Medical Postgraduate Conference, Hradec Kralove, Czech Republic. *Differential preferences in serosal homing and distribution of peritoneal B-cell subsets revealed by in situ CFSE labeling.*
(Oral presentation)

Awards:

2004. Az MTA Pécsi Területi Bizottsága és a "Dél-Dunántúl A Tudomány Támogatásáért" Alapítvány Tudományos Pályázata – II. Díj – *CD45RC Epitóp expressziójának vizsgálata monoklonális antitest és phage display technikával egér B-sejteken és előalakjaikon*

1 Introduction

1.1. The immune system

The function of the immune system is strictly based on the firm interplay between its hematopoietic and mesenchymal components. Although earlier its features were deciphered mainly at individual cellular level, now it is clear that understanding complex immunological processes can only be achieved through placing the observations into a realistic microenvironmental context that exists *in vivo*.

The major part of these efforts is to understand the structural development of secondary lymphoid organs (e.g. spleen [spl] or lymph nodes [LN-s]) where adaptive immune reactions take place, as well as the interplay between their vascular / stromal elements and cells generated in the primary lymphohematopoietic tissues (e.g. thymus and bone marrow).

Distinct organs of the immune system have different, although mutually complementary, functions. Accordingly, despite certain similarities in the course of their ontogenesis, they development significantly differ.

Evolutionary, the spleen is the oldest secondary lymphoid organ. As a solitary organ directly taking up antigens from the blood, its role is to provide adaptive immune response, a more effective reaction against pathogens compared to the innate immune reaction. Later the mucosal immune system developed, characterized with direct antigen uptake from internal surfaces, followed by the appearance of lymph nodes, where antigens are transported through the lymphatics draining the skin and also mucosal surfaces. This evolutionary scenario may also represent a developmental algorithm of the secondary lymphoid tissues during ontogenesis. It should be noted, however, that in spite of the appearance of distinct secondary lymphoid organs, the spleen retained its unique function in the defense against blood born pathogens as well as a central role in the homeostasis of adaptive immune system.

As the scope of our study was to determine the structural alteration of the spleen in the absence of one particular transcription factor and its consequences on the homeostasis of a unique B-lymphocyte subpopulation (called B-1a cells in mice), the structure and organogenesis of the rodent spleen deserves a more detailed discussion in three separate chapters.

1.2. Structure and development of the spleen

1.2.1 *Histological structure and lymphocyte distribution of the spleen in rodents*

The spleen is the largest, single secondary lymphoid tissue with the capacity to generate adaptive immune responses. Here, the immunological reactivity is preferentially targeted against blood-borne pathogens/antigens, and is manifested in diverse types of immune responses.

The lymphoid compartment of the spleen, the white pulp, is arranged around central arterioles, the terminal branches of the splenic artery [1]. The white pulp consists of the peri-arteriolar lymphatic sheeth (PALS, T-cell zone), the follicles (B-cell zone), and the marginal zone (MZ) forming the outermost edge of white pulp. In adult mice, the central arteriole is surrounded by PALS. Follicles are in direct contact with PALS, and together they form the central white pulp. The central white pulp is separated from – or connected to – the red pulp through the MZ (
Figure 1. a). Between the MZ and the central white pulp the marginal sinus (MS) is situated, a topographic element characteristic for rodent spleen. After crossing the central white pulp, portions of the terminal branches of central arteriole drain into the MS. However in humans an extensive branching can be observed both in the white pulp area and in the marginal zone, although no MS sinus exists [2]. In accordance with the spatial relation of the MS with the splenic circulation, MS/MZ is assumed to serve as the entry port of circulating lymphocytes from the blood stream to the spleen. One of the most abundant adhesion molecules expressed by the MS lining cells is mucosal addressin cell adhesion molecule 1 (MAdCAM-1), a widely used topographic marker in spleen histology, although MAdCAM-1 itself does not play a role in lymphocyte recirculation of the spleen.

The MZ surrounding the central white pulp is directly adjacent to the red pulp of the spleen. Two main cell types of hematopoietic origin reside in the MZ: the marginal zone B lymphocytes (MzB cells) and MZ macrophages.

MZ macrophages can be subdivided into at least two subpopulations, according to their scavenger receptor expression. The outer zone (red-pulp proximal) of macrophages expresses macrophage receptor with collagenous structure (MARCO) scavenger receptor, which has been shown important for the emergence of a lectin-like transmembrane protein, the SIGNR1 [3] [4]. The inner layer of macrophages is located on the white pulp side of the marginal sinus and its cells are referred to as metallophilic macrophages. Their distinguishing cell surface marker is sialic-acid-binding immunoglobulin-like lectin 1 (SIGLEC1,

sialoadhesin/Sn/CD169). The main role of these cells is the uptake of blood-borne antigens, and antigen presentation to T lymphocytes.

MzB cells have long been considered as resident, sessile cells of the MZ, with the main function of producing natural antibodies similarly to B-1a lymphocytes. [5]. However, it is now clear that natural antibodies are exclusively produced by B-1a cells [6]. Furthermore, a recent study using intravital imaging technique has shown that MzB lymphocytes shuttle extensively between the MZ and the follicles supporting their main role in transporting blood-borne antigens into the B-cell zone of the spleen [7].

The white pulp of the spleen is organized to provide and sustain T-cell dependent B-cell responses. Accordingly, the white pulp is separated into T-cell zone (PALS) and B-cell zone (follicles). The cellular origin of this separation is the presence of chemokine pattern in these regions maintained by the underlying stromal network. Thus the main chemokine of follicles is CXCL13 [8], and its corresponding receptor on naïve B cells is CXCR5. CXCL13 is mainly produced by follicule-specific stromal cells of unknown developmental origin, the follicular dendritic cells (FDC-s). Beside guiding B-cell distribution in the white pulp, FDC-s are indispensible in the central process of T-cell dependent B-cell response, the germinal center (GC) reaction [9]. The major chemokines of the PALS are CCL19 and CCL21 that are mostly produced by fibroblasts of the PALS [10]. Although dendritic cells (DC-s) of the PALS also produce these chemoattractants in a smaller amount, their major role is the activation of naïve T helper cells through antigen presentation, thus priming the T- cell dependent B-cell response. After activation, T helper cells downregulate CCR7 (the receptor for CCL19 and CCL21), which allows their migration toward the Fo-PALS boundary, where they further activate antigen-encountered B lymphocytes. Earlier it was considered that T-B interaction exclusively occurs on the follicule-PALS border. However, a subset of T helper cells has been identified later, with a hallmark of CXCR5 expression, allowing their entrance to Fo-s. There they play a pivotal role in guiding the GC reaction through interleukin 21 (IL-21) production. These T lymphocytes are referred to as follicular helper T cells (T_{FH}) [11]. In GC reaction, beside memory B cells, plasmablasts are formed that enter the red pulp through the so-called bridging channels [12], followed by the formation of long-lived plasma cells. The exact anatomic red-pulp location and cellular interactions of these long-lived plasma cells are still unknown.

1.2.2 *Splenic stromal microarchitecture*

The microarchitectural frame of the spleen is composed of region-specific fibroblast and endothelial compartments. These sessile stromal elements have far more sophisticated role in the immunological function of the spleen than merely providing a static tissue scaffold, and were largely neglected previously. However, more and more functions of these cells have been revealed recently.

Fibroblasts of distinct splenic regions are responsible for the production of homeostatic chemokines that are indispensible for the maintenance of the segregation of distinct T/B lymphoid compartments. Recent studies have also revealed that the fibroblastic scaffold of the spleen forms the so called conduit system. These are channels of various diameter in different regions of the spleen, containing extracellular matrix. This heterogeneous extracellular matrix forms the reticular fiber network within the conduits, in the center of which fibrillar collagens can be found, ensheated by a basement membrane layer and microfibrillar proteins [13]. Their main role is to provide a directed gradient of homeostatic chemokines for the migration of lymphoid cells in the stroma of the spleen.

Endothelial cells of distinct phenotypes line the venous sinusoid system of the red pulp, and may be involved in the formation of MS.

The endothelial cells as well as the fibroblasts are considerably heterogeneous, and different subtypes are arranged at distinct part of the spleen. In our institute, numerous monoclonal antibodies have been produced to identify distinct subsets of stromal cells. Among these, IBL-10 and IBL-11 are fibroblast-, IBL-7/1 and IBL-9/2 are endothel-specific antibodies [14], [15], providing differential labeling of the distinct subsets of the respective stromal cells (the nomenclature of these monoclonal antibodies is based on a simple convention: IBL stands for the earlier name of our institute, “Immunological and Biotechnological Laboratory”, and the ensuing number refers to the hybridoma clone producing the respective monoclonal antibody). Although the exact antigen-specificity of several of these antibodies is still unknown, they became invaluable topographic markers and proved useful in determining differential developmental features of distinct territories of the spleen.

Figure 1. schematically demonstrates the tissue organization of the spleen, and territory-restricted localization of stromal cells of distinct regions in relation to topologic markers.

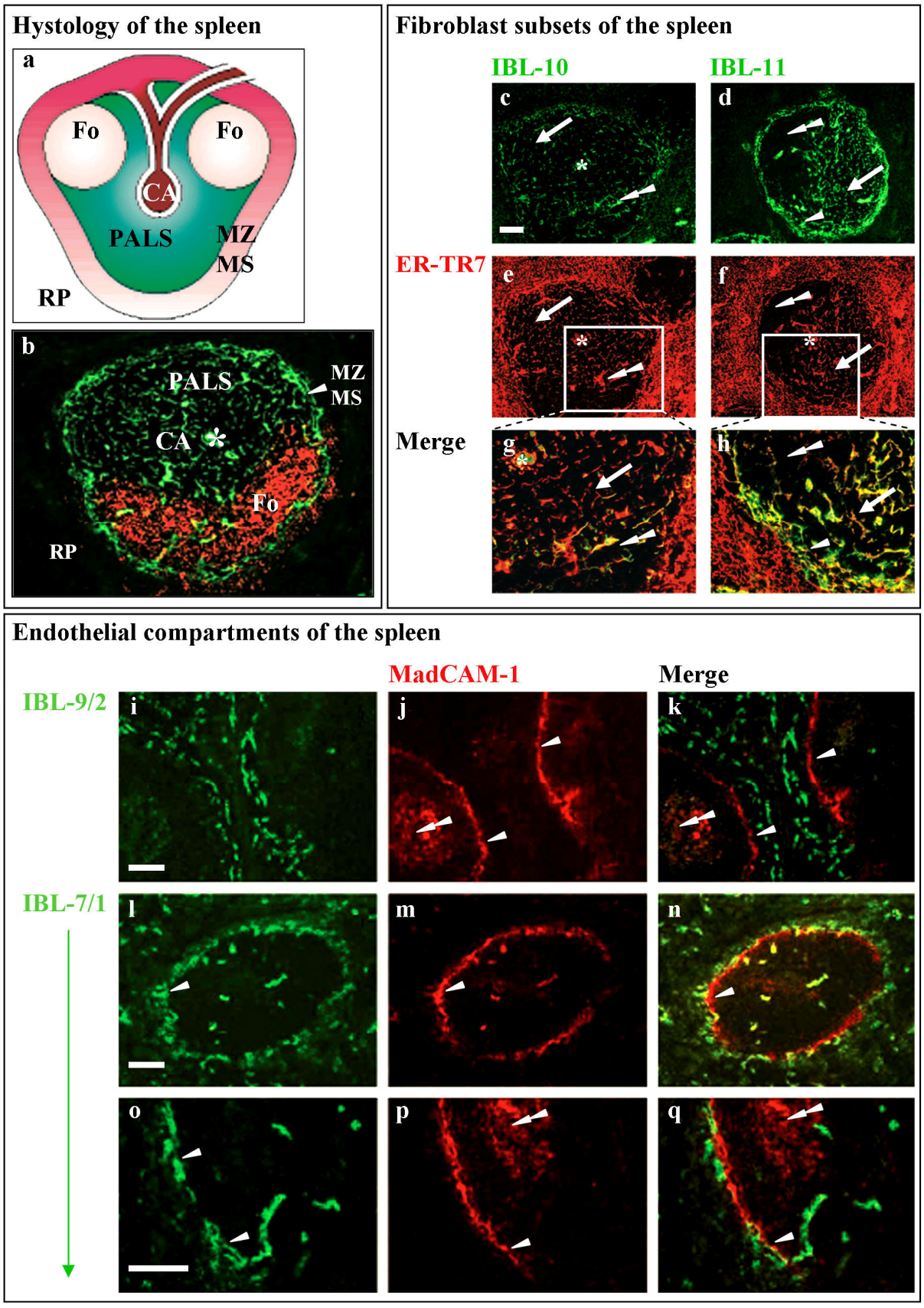
Hystology of the spleen
a
Fo
Fo
CA
PALS
MZ
MS
RP
b
PALS
MZ
MS
CA
Fo
RP
Fibroblast subsets of the spleen
IBL-10
IBL-11
c
d
ER-TR7
e
f
Merge
g
h
Endothelial compartments of the spleen
MadCAM-1
Merge
IBL-9/2
i
j
k
IBL-7/1
l
m
n
o
p
q

Figure 1. Histology and stromal compartments of the spleen. The white pulp as well as the red pulp are abundant in region-specific stromal cells of different phenotypes.

Histology of the spleen: a, The white pulp is arranged around central arterioles (CA and/or asterisk throughout the figure), the terminal branches of the splenic artery. The T-cell zone (PALS) is situated immediately around the CA. The terminal branches of CA, after crossing the white pulp, drain either into the venous sinusoids of the red pulp (RP), or the marginal sinus (MS). PALS and B-cell zones (follicles, Fo) are surrounded by the MS, which is connected with the RP through the marginal zone (MZ). b, Immunofluorescent image represents the clear separation of distinct zones of the white pulp. The follicle is represented by red fluorescence, achieved with labeling of FDC-s. The PALS, the MS and MZ are represented by green fluorescence, implemented with the labeling of a subtype of fibroblasts, underlying these areas.

Fibroblast subsets of the spleen (c-h): Fibroblasts represent essential stromal elements of the spleen by producing homeostatic chemokines, responsible for the PALS (arrows)-follicle (double arrowheads)-MZ (arrowheads) segregation in the spleen, and maintaining their concentration gradient through the formation of the conduit system. The fibroblast network shows a considerable heterogeneity in the spleen as revealed by distinct fibroblast-specific monoclonal antibodies (mAb-s). ER-TR7 mAb (e, f,) is a widely used general reference marker of the splenic fibroblasts, probably recognizing conduit material in every region of the spleen. Fibroblast subsets expressing antigens recognized by IBL-10 mAb (c, g), are abundant in the Fo-s, as shown by the co-localization of the IBL-10 and ER-TR7 signals in these regions (g), appearing as yellow fluorescent areas. This juxtaposition is less obvious in the PALS indicating the paucity of these fibroblast subsets there. On the other hand, IBL-11 mAb labels fibroblasts situated in the PALS and those forming the circumferential reticulum, the fibroblastic frame of the MZ (d, h), but absent from the Fo-s. Pictures g and h represent the inset of pictures e and f, respectively after digital merge with c and d, respectively. Bar corresponds to 100 μm.

Endothelial compartments of the spleen (i-q): Sinusoids also show considerable heterogeneity, revealed with mAb-s IBL-9/2 (i,k) and IBL-7/1 (l,n,o,p). Using these mAb-s together with MAdCAM-1 as a topologic marker for MS-forming cells (arrowheads) and, somewhat less intensively, for the FDC-s (double arrowheads, j,m,p and k,n,q images) at least two distinct endothelial subsets are identified. IBL-7/1^{lo}/IBL-9/2 $^{+}$ endothelial cells are positioned deep in the red pulp, not overlapping the MAdCAM-1^{+} MS-forming cells. However, IBL-7/1^{hi}/IBL-9/2 $^{-}$ endothelial cells are juxtaposed with the MS, may even contribute to MS, as clearly seen in picture **q** (arrowhead). Bars correspond to 10 μm. (images were rendered from [1], [16]; [17])

1.2.3 *Organogenesis of the spleen*

The complex ontogenesis of the spleen from its mesenchymal anlage involves many cell-intrinsic factors (mainly transcription factors) as well as receptor-ligand pairs mediating the effect of cellular interactions between stromal precursors and haematopoietic cells [18]. Some of these molecules and processes are involved in the development of other secondary (or even tertiary) lymphoid tissues, while others are spleen-specific. Although there have been many works published recently addressing the function and hierarchic organization of these factors, their exact relationship are still largely unknown.

The organogenesis of the spleen can be divided into three main phases. During the first embryonic phase, the condensation of the mesenchymal cells of the dorsal mesogastrium begins, forming the splenic anlage, initially situated dorsal to the stomach [19]. Subsequently, during the second phase, hematopoietic cells colonize this anlage. This process is accompanied by the early segregation of the red pulp and the rudimentary periarteriolar white pulp, as well as the asymmetric growth of the spleen, resulting in its anterior-leftward migration. At the second half of this phase an extensive vascularization of the red pulp begins. During the third phase, around birth, mature lymphocytes colonize the periarteriolar region. Initially, these cells mainly consist of B lymphocytes accumulating around the central artery that are gradually displaced by T lymphocytes during the first postnatal week. After this stage, the B cells converge into follicles that are formed together with the underlying FDC network and with the surrounding MZ. Thus, a significant part of the rodent splenic development takes places after birth [2].

In these phases of the splenic development several transcription factors are involved. According to the timing of and their mutual effect on their appearance in the anlage, a hierarchic scheme has been proposed on the role of distinct transcription factors in splenic organogenesis. Although this scheme is rather straightforward, it should be kept in mind that many members and interactions of these processes are still unknown. This scheme is represented by Figure 2. As a general feature of this transcriptional network, it can be assessed that there are many factors involved in early spleen specification that belong to distinct protein families. Although they act at different stage of the early spleen development, and although there are several parallel pathways described, these factors are non-redundant,

and the isolated absence of any of them leads to asplenia [20], [21], [22], [23], [24]. On the other hand, the lack of later-arising factors, such as Nkx2.3 [25], [26], [27], or external regulators of tissue development, such as lymphotoxin alpha (LTα) and lymphotoxin beta receptor (LTβR), leads to the altered development of distinct tissue compartments (fibroreticular, as well as distinct endothelial compartment) of the spleen, without causing asplenia [28], [29], [30].

The fibroreticular and endothelial alterations in Nkx2.3 KO mice have been well characterized and are detailed in the following chapter.

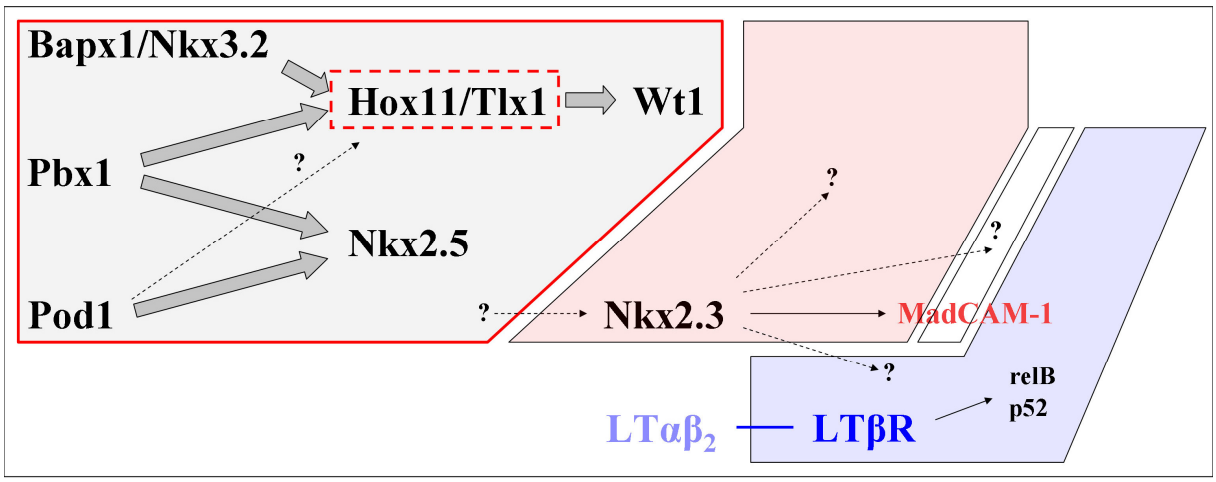

Figure 2. Intra-and extracellular master regulators of the development of the stroma of the spleen. Several factors participating in the formation of the spleen have already been identified. In this figure, transcription factors are in black, extracellular regulators are written in blue letters, and the single, already identified target of Nkx2.3 homeodomain (HD) transcription factor, MAdCAM-1 is shown in red. The transcription factors in the red-lined polygonal area are indispensible for the early specification of the spleen, and the lack of any of them leads to asplenia. In this network, in a pleiotropic fashion, one transcription factor may be involved in the regulation of more transcription factors. Other factors (Nkx2.3 HD transcription factor or signaling through LTβR) may be lacking without causing asplenia, but their absence influences the development of the spleen in a tissue-compartment dependent manner. The regulatory mechanism of the Nkx2.3 is unknown, and the only identified target gene of Nkx2.3 is MAdCAM-1, which, in turn, is also regulated by LTβR signaling through relB and p52, two components of the alternative NF-kB transcription pathway. Red-filled polygonal area indicates that lack of Nkx2.3 transcription factor brings about major effect in the development of red pulp with slighter alteration in the white pulp (blue-filled polygonal area), whereas alteration of the LTβR signaling at any level mainly affects the white pulp. In both cases the marginal zone together with the marginal sinus (schematically represented as black-lined white rhomboid positioned between the red and blue polygons) is severely affected.

1.2.4 *Defective stromal (endothelial and fibroreticular) development of the spleen in Nkx2.3 KO mice*

Earlier publications in Nkx2.3 KO mice describing abnormal T/B-cell zone separation reported the lack of haematopoietic cellular components of the MZ, and the gross macroscopic alteration of the red pulp of the spleen [25], [26], [27] prompted the detailed examination of splenic stromal elements in these mutants. Two separate publications revealed severe developmental alterations in distinct endothelial as well as fibroreticular compartments of Nkx2.3 KO mouse spleen using endothel- and fibroblast-subset specific monoclonal antibodies described in section 1.2.2 [16], [17].

Figure 3. represents the complex endothelial alterations caused by the lack of Nkx2.3 HD transcription factor. The red pulp venous sinusoidal compartment, identified by their strong IBL-9/2 staining and characterized by deep-red pulp localization, is completely absent from mutant mice (Figure 3. c). Furthermore, IBL-7/1^{hi}/IBL-9/2 $^{-}$ endothelial subset normally closely associated with MS, or even participating in the formation of the lining of MS, looses its preferential localization in red pulp area close to the white pulp, and nearly completely confined to the subcapsular regions of the mutant spleen (Figure 3. a). IBL-7/22 labeling – as a topologic marker mainly used for identifying the MS - also reveals the lack of this zone in mutants (Figure 3. b).

The fibroreticular meshwork of Nkx2.3 KO mutant mice also showed significant alterations as revealed by the staining with the general fibroblast marker (Figure 4. a, b), follicular- (Figure 4. c, d), and PALS-specific (Figure 4. e, f) fibroblast markers, the later also delineating the circumferential reticulum (fibroblastic frame of the MZ) in wild-type (wt) mice. Beside disorganized fibroblastic network, mutant spleen lacks fibroblast subset normally localized to follicles. Additionally, disorganization of the PALS-specific, IBL-11^{+} fibroblast, together with the clogged organization of FDC-s, results in the loss of complementary arrangement of FDC-s and fibroreticular meshwork of the PALS in mutants (Figure 4. g, h).

1.

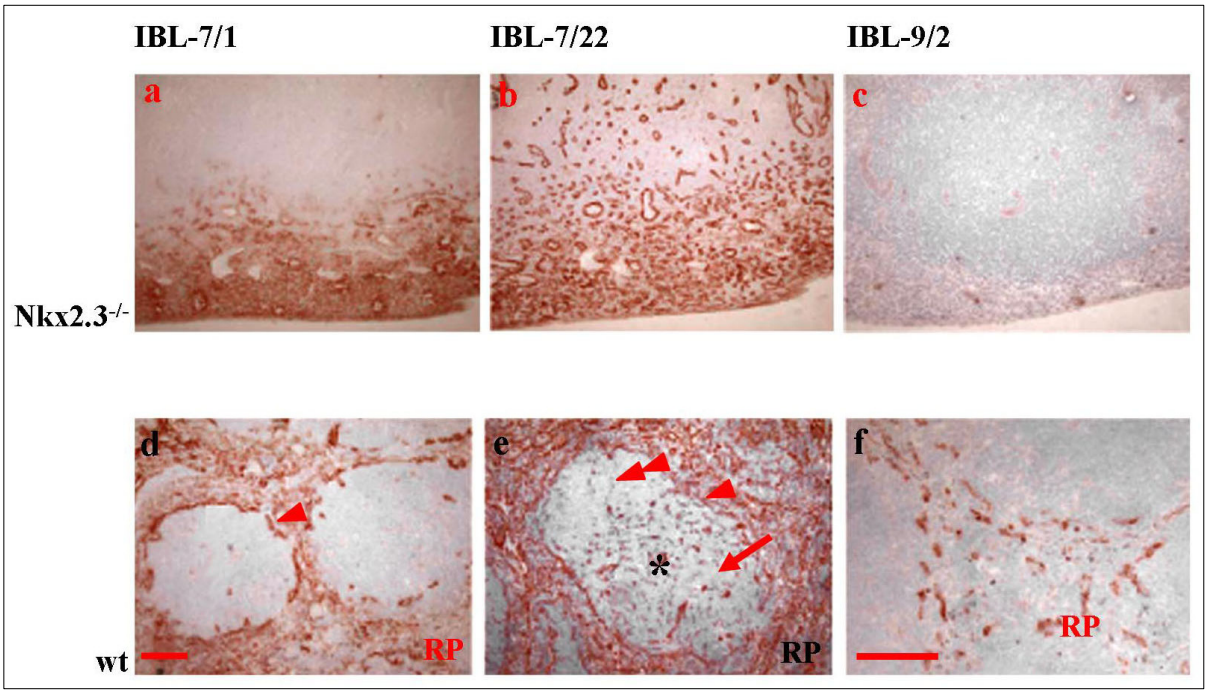

Figure 3. Altered arrangement of distinct endothelial compartments of the spleen in Nkx2.3 KO mice. The lack of Nkx2.3 results in the disruption of MS (arrowheads, compare a, b, with d, e,) and the diminished development of red pulp sinus network (RP), with the complete lack of endothel subsets expressing antigen recognized by IBL-9/2 mAb (c,f). Arrow represents the PALS, double arrowhead represents the follicle (image rendered from [17]). Scale bars, 100 μm.

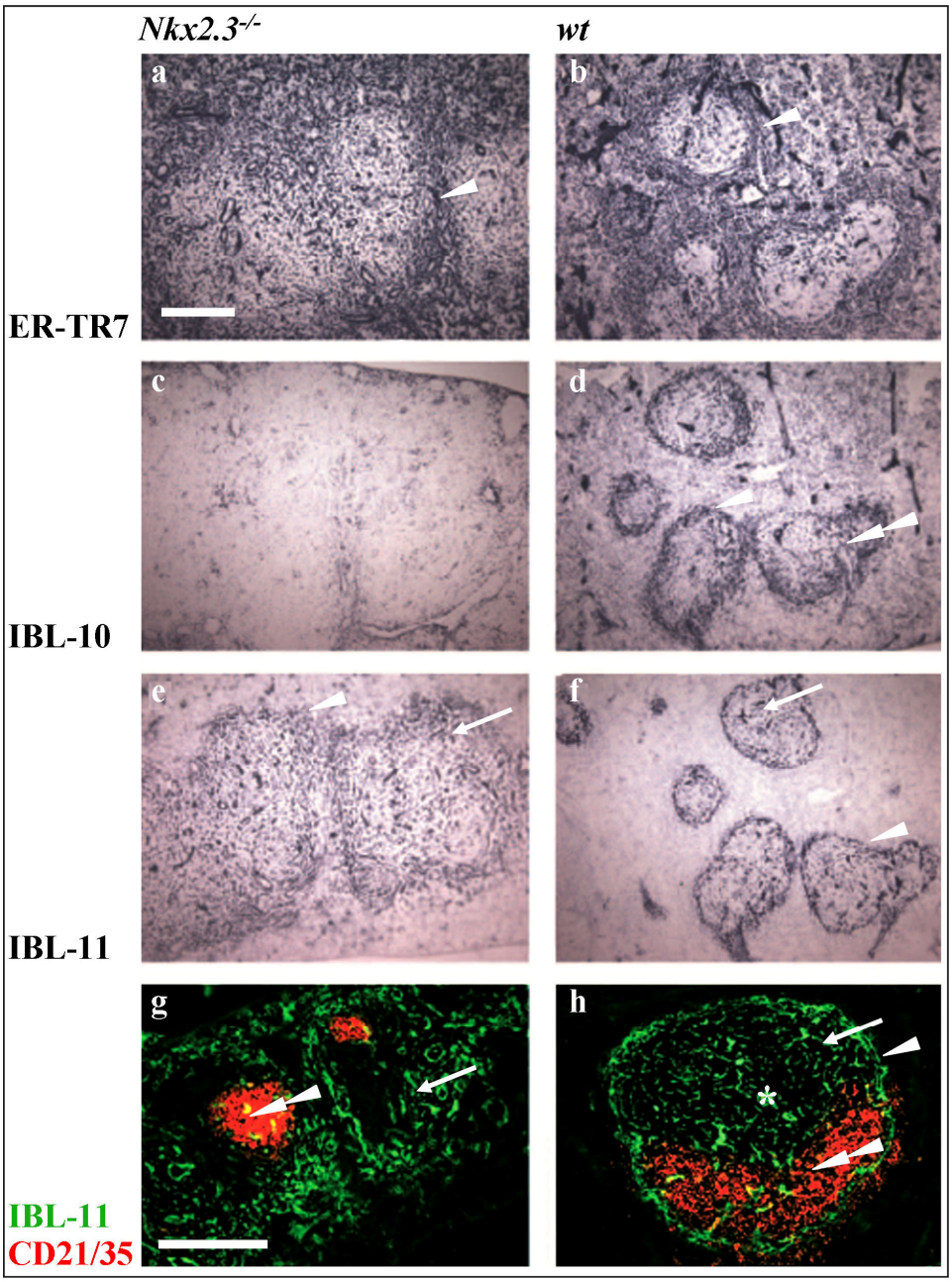

Figure 4. Effect of the lack of Nkx2.3 transcription factor on the fibroreticular network of the spleen. The lack of Nkx2.3 transcription factor results in disturbed organization of the fibroreticular network of the spleen as indicated by the diffuse staining pattern with ER-TR7 mAb (a, b), the lack of IBL-10 reactivity (c), normally localized to the follicles (d), and absence of compartmentalized IBL-11 reactivity (e), normally labeling the PALS (arrow) and the circumferential reticulum (arrowhead, f). Furthermore, the complementary localization of IBL-11$^+$ fibroblasts with FDC-s (double arrowheads, h), as revealed by IBL-11 and CD21/35 double staining, is also disturbed. This is jointly attributed to disorganized fibroreticular meshwork and clogged arrangement of FDC-s (g). Size bars, 100 μm. Images are rendered from [16].

1.3. Functional classification of the molecules and cells of the immune system – innate and adaptive immunity

According to their specificity and their role in the complex process of immune response, molecules and cells of the immune system can be classified into two distinct groups: (1) those molecules and cells, that first encounter with invading pathogenic organisms make up for the innate immune system, whereas (2) those with the help of the innate immune system react to pathogens in an antigen-specific manner, amplify the overall efficiency of the immune response and form immunological memory, belong to the adaptive immune system [31]. This classification also reflects the appearance of the components of the immune system during evolution, as cells and molecules of the innate immune system constitute a more ancient system.

The innate immune system provides the first line of defence for an organism against invading pathogens. In accordance with this role, the response of this system is prompt, and is able to act against a wide range of pathogens in a non pathogen-specific manner. The receptors of the cells of the innate immune system are able to recognize a wide range of molecular patterns that are conserved among various pathogens, thus providing a general response against distinct pathogens. Consistently, the major receptors of the innate immune system fulfilling these roles are called pattern recognition receptors that are encoded by genes without previous recombination, i.e. by genes in germline configuration.

In contrast to innate immunity, one of the main distinctive features of the adaptive immune system is antigen specificity. The central process of the maturation of lymphocytes, the cellular components of the adaptive immune system of haematopoietic origin, is the formation of antigen receptors (B-cell receptor [BCR] and T-cell receptor [TCR]) through homologous recombination in the antigen-receptor genes. Lymphoid precursors expressing antigen receptors encoded by the formerly rearranged antigen-receptor genes undergo sequential stages of positive and negative selections, a process better characterized in T lymphocyte maturation. As a result, lymphocytes bearing either non-functional or self-reactive antigen receptor are eliminated, thus only self-tolerant, immunocompetent lymphocytes may enter the mature lymphocyte pool. All these events, leading to the formation of mature B and T lymphocytes, take place in the primary lymphoid tissues, i.e. the bone marrow and thymus, respectively. A further distinctive feature of the adaptive immune system is that upon activation, the respective antigen receptors of B lymphocytes undergo affinity maturation; furthermore, the cells are able to form memory. During affinity

maturation further changes are introduced in the antigen-receptor at genome level. Thus, upon first encounter with a given antigen, adaptive immune response (referred to as primary immune response) becomes more effective along its process. Additionally, due to the formation of memory, further encounter with the same antigen elicits a more effective response than the primary one.

It should be noted, however, that the distinction between innate and adaptive immune system is not completely clear, especially with the later description of two group of cells, the innate lymphoid cells (ILC-s) [32] and the innate-like lymphocytes (ILL-s) [33]. Identification and characterizations of cells belonging to either ILC-s or ILL-s have not only blurred the boundary between innate and adaptive immunity, but also highlighted that the immune system – besides combating infections - plays an important role in tissue repair and homeostasis, and defense against autoimmunity, chronic inflammatory diseases and malignancies. Furthermore, some of these "mobile" elements of the immune system are indispensable for the development of stromal or vascular elements of distinct secondary lymphoid tissues.

Earlier natural killer (NK) cells were considered the only effector cells of the innate immune system of lymphoid origin [34]. Recently, however, several other cells derived from lymphoid progenitors have been identified and, together with the NK cells, are now classified as members of ILC-s. Beside lymphoid origin, the ILC-s share further common developmental features: they lack TCR or BCR locus rearrangement, and all of them requires inhibitor of DNA binding 2 (Id2) protein for their commitment [35], [36]. NK cells (the first identified group of ILC-s) play a major role in the immediate defense against virus-infected and tumor cells. The second group (that of the retinoic acid-related orphan receptor γ t [RORγt] dependent ILC-s) participate in the organogenesis of lymph nodes, Peyer's patches, and – postnatally - the isolated lymphoid follicles (ILF-s) in the gut (lymphoid tissue inducer [LTi] cells). Other members of this subgroup of ILC-s (the ILC17 and ILC22 cells) are named after the major IL that they produce, and have protective role under inflammatory conditions of the gut. The third group of ILC-s, the so called type 2 ILC-s have been found responsible for regulating process against airway helminthiasis, and respiratory allergic reactions and play important role in wound healing [32].

In contrast to ILC-s, ILL-s lie on the "adaptive side" of the blurred border between the innate and adaptive immune system, in a sense that, similarly to conventional B and T lymphocytes, during their development the antigen receptor gene (BCR or TCR) is rearranged. However, their BCR and TCR repertoire - mainly resulting from the evolutionary

conserved and limited V fragment usage – is rather small, compared to that of conventional (adaptive) lymphocytes. Furthermore – also in contrast to their conventional counterparts – upon maturation, no untemplated nucleotide (N) addition occurs at the V-D-J junction of their antigen receptors. Thus, in spite of the antigen receptor rearrangement, this semi-invariant usage of receptors, together with their preferential peripheral tissue localization, as well as the pre-activated phenotype, make these cells functionally similar to cells of the innate immune system. ILL cells comprise the CD1d-restricted natural killer T (NKT) cells, the epidermal localized γδ T cells, and the natural antibody producing B-1a cells, which will be described in more details in the following section [33].

1.4. B-1a cells - somewhere between the innate and adaptive immune system

B-1a cells represent a unique lymphocyte population. These cells mainly accumulate in serosal cavities and also dwell in the spleen, and in mice express CD5 which is unique among B-lymphocyte subsets [37].

As these B cells appear first during ontogeny among peripheral B-cell subsets, they were initially referred to as B-1 cells distinguishing them from the later arising follicular (or B2) B lymphocytes. Another, minor B-1 cell subset was discovered later in the murine peritoneal cavity, sharing many phenotypic properties with the originally described $CD5^+$ B-1 cells, except for the expression of CD5 itself. In order to distinguish these subsets, the originally described $CD5^+$ B-1 cells was referred to as B-1a cells, and the smaller $CD5^-$ "sister" population was named B-1b cells. Further extensive studies revealed essential developmental and functional differences between these two populations [38].

A distinctive developmental feature of B-1a cells is that their major pool is generated during fetal life. Several embryonic tissues have been shown to harbour precursors with B-1a potential and, based on irradiation chimera systems, B-1a cells are most efficiently reconstituted in adult mice from haematopoietic precursors of fetal liver origin. As a result of this extensive potential for B-1a cell formation, it was assumed initially that fetal liver is the only niche able to produce B-1a cells, and B-1a cell formation does not takes place in adult bone marrow. However, it is now clear that B-1a specific precursors also persist in the bone

marrow [39]. Nevertheless, its contribution to the formation of B-1a cells is limited under steady state conditions, possibly by a feedback regulation of the self-maintaining B-1a cell pool that is already formed during the embryonic life [40].

Similarly to other B-cell subsets, B-1a cells undergo BCR gene rearrangement during maturation, and subsequently express BCR. In this term, these cells belong to the adaptive immune system. However, they produce natural antibodies that are formed without any obvious previous antigen exposure and this antibody production is independent from the presence of T lymphocytes [41], [42], [43]. Natural antibodies have low affinity binding against a wide range of microbial antigens largely conserved among species, as well as cross-reactive features targeting them against self antigens. These antibodies thus represent a preformed, immediate humoral-like defense mechanism against invading pathogens, and in this term they have an innate-like function [44], [45]. On the other hand, their antibody production and survival depends on the spleen, and in this context as well, they are rather similar to the adaptive immune system [6], [46], [47], [48], [49], [30],[50].

1.5. Role of the spleen in the homeostasis of B-1a cells

During ontogeny, a unique mutual relationship is established between the spleen and B-1a cells.

In rodents around birth, B-1a B cells accumulate around the central arteriole after their production in fetal hematopoietic tissues. It is assumed that these cells play an important role in the postnatal development of the splenic FDC-s. By the 7-8 postnatal day these cells are gradually displaced by T lymphocytes forming the PALS [2]. Mature follicular B cells also accumulate in the spleen, and although the absolute number of B-1a cell in the spleen remains significant, their relative frequency continuously decreases. In parallel with these processes, B-1a cells first appear in the peritoneal cavity (and other serosal cavities) on the 8. postnatal day where this population continuously accumulate, gain adult-type phenotype and antigen-receptor repertoire with the expression of CD11b marker and the appearance of V_H11-bearing BCR-s, respectively [51].

After their formation during embryonic life, B-1a cells represent a self-maintaining population [37], [52], [53], [54]. Although it has been shown recently that adult bone marrow retains the potential of B-1a cell formation [55], under steady state conditions B-1a cell

population is overwhelmingly maintained by self-division, and B-1a influx from the bone marrow is negligible [40]. Importantly, the self-renewal capacity of these cells largely depends on the spleen. It has been demonstrated that the peritoneal B-1a cell frequency in HOX11 homeodomain transcription factor KO (asplenic) mice is largely reduced [49]. In n-ethyl-n-nitrosourea (ENU) - induced LTα mutant mice the lack of marginal zone and clear T- and B-cell zone separation of the spleen is also accompanied by the reduction of peritoneal B-1a cell frequency [30]. Prompt reduction of peritoneal B-1a cells can also be observed after splenectomy of wild-type mice as well, and affects BCR repertoire in immunoglobulin light chain (IgL) transgenic (L) mice [48]. Recurrent microinfarction of the spleen in mouse model of sickle-cell disease results in the continuous development and progression of functional asplenia with disturbed white pulp structure, involving the disorganization of the PALS, follicles and MZ. This process is accompanied by the reduction of the frequency of splenic B-1a cells together with the decrease of immunoglobulin A (IgA) secreting plasma cells in the gut [50], a possible derivate of peritoneal B-1a cells [56], [57], [58].

Together these results suggest that, after playing an important role in the formation of splenic white pulp stroma after birth, the maintenance of B-1a cell is largely dependent on the spleen possibly mainly by their recirculation there for the acquisition of survival / division signals. However, the nature of this putative signal still remains to be determined.

2 The implication and aim of the study

The pathogenic role of B-1a cells has been suggested in several mouse models of autoimmunity as well as their possible relationship with distinct haematological malignancies (especially $CD5^+$ B-CLL) [37], [59]. Thus understanding the homeostasis of B-1a cells under steady state and pathologic conditions seems reasonable.

Although it has been demonstrated that the spleen plays an indispensable role in the maintenance of B-1a cells, the exact cell type or tissue compartment responsible for B-1a homeostasis is not known. Therefore animal models with distinct alteration in splenic structure may prove useful in understanding the microenvironmental requirement of the self-maintenance of B-1a cells. However, precise assays also need to be developed in order to monitor steady-state B-1 B-cell homeostasis, with as little interference with the physiological conditions as possible.

Therefore we used the Nkx2.3 KO mouse model, with already described splenic stromal alterations. In this work, before characterizing the B-1a cell homeostasis we further investigated the developmental characteristic of the vascular compartment of the spleen in mutant mice. Accordingly my thesis is arranged around 3 main blocks: 1. Despite the endothelial alterations described so far, accumulation of lymphocytes in the mutant spleen further prompted us to examine changes in the development of its vasculature and lymhocyte homing events in details. 2. Subsequently, with the introduction of a novel *in situ* fluorescent labeling method, I sought novel analytical procedures allowing systemic evaluation of B-1 cell composition and distribution. 3. Finally, I aimed to determine the changes of B-1a cell homeostasis in Nkx2.3 KO mice and their possible causes through comparing peritoneal B-1a cell compartment of mutant and wt mice over time, and performing peritoneal cell transfer experiments, respectively.

3 Materials and Methods

3.1 Mice

Nkx2.3$^{-/-}$ mice from a 129Sv x B6 mixed background were backcrossed with BALB/c mice (obtained from Charles River Laboratories, Budapest, Hungary) through 14 generations and genotyped using conventional duplex PCR method amplifying Nkx2.3 and neomycin resistance gene, a part of the targeting construct used for knocking out the Nkx2.3 gene [26]. C57BL/6 and 129Sv Nkx2.3 mutants were maintained at the Technical University of Braunschweig (Braunschweig, Germany). For homing and peritoneal cell transfer studies, BALB/c mice from our faculty's specific pathogen-free breeding unit were used as a lymphocyte donor for adoptive transfer. All procedures involving live animals were conducted in accordance with the guidelines set out by the Ethics Committee on Animal Experimentation of the University of Pécs.

3.2 Antibodies and reagents

Rat anti-mouse immunoglobulin M (IgM) and fibroblast-specific mAb producing hybridoma (clone: IBL-16 and IBL-11, respectively) were developed in our laboratory. Rat hybridoma cell lines secreting anti-CD3 (KT-3), anti–MAdCAM-1 (MECA- 367), L-selectin/CD62L (MEL-14), anti-mouse CD5 (53-7.3) and B220 (RA3-6B2) were obtained from the American Type Culture Collection and used either as a hybridoma supernatant or a fluorescein-conjugated reagent. Horseradish peroxidase conjugated rabbit anti-mouse IgM and immunoglobulin G (IgG) were purchased from Zymed. PE-conjugated anti-mouse CD21/35 mAb (clone 7G6), PE-conjugated anti-mouse CD11/b (Mac-1, clone: M1/70), anti-mouse CD43 (clone: S7), anti-mouse CD21 (clone 7G6), anti-mouse CD23 (clone: B3B4), anti-mouse immunoglobulin D (IgD) (clone: 217-170) MECA-79 mAb against peripheral node addressin (PNAd), and FITC- labeled and PE-conjugated goat anti-rat IgG were purchased from BD Biosciences (Soft Flow Kft, Pécs, Hungary). Goat Abs against CCL21 chemokine and NorthernLights 557-conjugated donkey Ab against goat IgG were obtained from R&D Systems (Biomedica Hungary Kft, Budapest, Hungary). Biotinylated rat mAb against mouse

IgM was produced in our laboratory from B7.6 clone. Goat anti-mouse IgM–HRP conjugate was produced by Invitrogen (Csertex Kft, Budapest, Hungary). Affinity-purified rabbit polyclonal Abs against HEC-GlcNAc6ST sulfo-transferase [60] were provided by Dr. N. H. Ruddle (Yale University School of Medicine, New Haven, CT) and were detected with FITC-conjugated goat anti-rabbit IgG (Sigma-Aldrich). Streptavidin-Alexa Fluor 350 and streptavidin-Alexa Fluor 488 conjugates were purchased from Invitrogen. LTβR–Ig (lymphotoxin beta receptor – immunoglobulin) fusion protein was provided by Dr. J. L. Browning (Biogen Idec Cambridge,MA) and was injected in newborn Nkx2.3KO mice as described previously [17]. Pooled human IgG was used as control.

3.3 Chemicals

Intracellular fluorescent dye carboxyfluorescein diacetate succinimidyl ester (CFSE) was obtained from Invitrogen (Csertex Ltd, Budapest, Hungary). Dimethyl sulfoxide (DMSO) was purchased from Sigma–Aldrich Ltd, Hungary, Budapest. LPS (O:55 serotype) was a kind gift of Dr Béla Kocsis (Department of Medical Microbiology and Immunology, University of Pécs, Hungary)

3.4 *In situ* CFSE labeling

CFSE was dissolved in DMSO (5 mg/ml) and diluted to 25 or 50 μg/ml in sterile PBS without Ca^{2+} and Mg^{2+} ions. Of this solution, 1 ml per 20 g weight for mouse was injected intraperitoneally (i.p.) slowly over the period of 20 s using G27 needle affixed to a 1 ml insulin syringe. After releasing the hind legs, the abdomen of mice was gently tapped to ensure even distribution of labeling mixture, and the mice were returned to their box. After various time points, the mice were sacrificed and the frequency and fluorescence intensity of CFSE-labeled cells in the peritoneum, pleural cavity, and in various peripheral lymphoid organs were investigated.

3.5 Intraperitoneal LPS administration

LPS was dissolved in sterile PBS without Ca^{2+} and Mg^{2+} ions at a concentration of 100 μg/ml. Two hundred and fifty microliter of this solution was injected i.p. to the mice 2 h after intraperitoneal CFSE administration.

3.6 Single-cell suspension preparation

Lymphocytes were isolated from the spleen and lymph nodes by tearing apart the organs between the frosted ends of two microscopic slides and filtered through a 70-μm pore-size cell strainer. Peritoneal cells were isolated by flushing and regaining 4-5 ml incomplete DMEM from the peritoneal cavity of mice through a substernal incision. Pleural cells were isolated through a right parasternal incision by flushing and regaining 1 ml incomplete DMEM from the pleural cavity. Importantly, care was taken to keep the diaphragm intact in order to avoid the contamination of pleural samples with peritoneal cells. Lymphocytes were isolated from the spleen and lymph nodes by teasing apart the organs between the frosted ends of two microscopic slides and filtered through a 70-μm pore-size cell strainer.

3.7 Flow cytometry

Isolated cells from LN-s and spleen were incubated with a mixture of fluorescein-labeled anti-B220 and biotinylated anti-CD3 or anti-CD62L, mAb in the presence of 2.4G2 anti-CD16/32 mAb. The biotinylated mAbs and the biotinylated cells in homing studies were detected with PE-streptavidin. Peritoneal cells were incubated with a cocktail of Alexa 647-labeled anti-mouse B220, PE-conjugated anti-mouse Mac-1/CD11b, biotinylated anti-mouse CD5 and, in the case of peritoneal cell phenotyping, one of the following unlabeled rat anti-mouse antibodies: anti-IgM, anti-IgD, anti-CD21, anti-CD23, anti-CD43. The biotinylated anti-mouse CD5 was detected with PE–Cy5–streptavidin, and the unlabeled rat anti-mouse antibodies were detected with FITC-conjugated goat anti-rat-IgG. Dead cells were excluded based on their light scattering properties. At least 20,000 live cells were collected by a BD

Biosciences FACSCalibur cytometer and analyzed using the BD Cell-Quest software, or WinMDI 2.8 software.

3.8 Immunohistochemistry and immunofluorescence

Single and dual-label immunofluorescence and immunohistochemical procedures were described in [17]. For control staining normal rat IgG at 10 μg/ml concentration was used. After mounting the sections were viewed under an Olympus BX61 fluorescent microscope. The acquisition of digital pictures with a charge-coupled device camera was performed using the analySIS software.

3.9 In vitro CFSE labeling of lymphocytes isolated from peripheral lymph nodes, and adoptive cell transfer of the labeled cells

Lymphocytes from peripheral lymph nodes (pLN-s) or mesenteric lymph nodes (mLN-s [mesenteric lymph nodes]) were isolated and labeled with CFSE (Invitrogen) or sulfo-N-hydroxysuccinimide biotin ester (Sigma-Aldrich) as described in [61]. For lymphocyte homing studies, 200 μl cell suspension at 5 x 10^7 CFSE-labeled cells was injected intravenously (i.v.) in the tail vein, followed by the removal of the spleen at various intervals. The distribution of labeled cells was tested by immunofluorescence using anti-PNAd or IBL-11 mAb against white pulp fibroblasts [14] in conjunction with PE-labeled anti-rat IgG. For competitive homing, two different cellular labeling procedures were used in which the CFSE-labeled cells were subsequently incubated with purified MEL-14 IgG or IBL-10 control rat mAb. After washing, cells were counted and mixed at 1:1 ratio with biotinylated cells as reference population, followed by the i.v. injection of mixed cells. Mice were sacrificed 30 min after the injection, and their distribution of CFSE-labeled and biotinylated lymphocytes in different lymphoid tissues was determined by flow cytometry or immunofluorescence. To be able to perform these measurements, biotinylated cells were labeled with streptavidin-phycoerythrin (BD Biosciences) following the single cell suspension preparation from the isolated tissues. The CFSE:biotin ratio of the cells in lymphoid organs was calculated following the normalization of labeled cell frequencies with the preinjection CFSE:biotin

ratio; thus, the CFSE:biotinylated cell ratio recovered from each organ was divided by the CFSE:biotinylated cell ratio in the preinjection cell mixture.

3.10 *In vitro* CFSE labeling of peritoneal cells, and peritoneal cell transfer

Peritoneal cells were isolated by lavage and the cells were incubated at a 10^6/ ml cell density in either 1 μg/ml, or 6 μg/ml CFSE dissolved in PBS/0.1% BSA for 10 min at 37°C on a rotator. The appropriate working concentration of CFSE during the labeling was chosen according to the respective experiments performed. Reaction was stopped by washing the cells with ice-cold complete DMEM medium. A total of 5 x 10^6 CFSE-labeled cells per recipient were i.p. injected to mice.

3.11 ELISA

ELISA plates (Nunc Maxisorb) were coated with 23 μg/ml Pneumovax-23, with 10 μg/ml phosphorylcholine or with 5 μg/ml monoclonal rat α-mouse IgM (clone IBL-16) to measure the relative serum level of pneumococcus polysaccharide (PPS)-, phosphorylcholine-specific IgM, IgG and that of total IgM antibodies, respectively. Diluted sera of mice were then added, followed by the addition of horseradish peroxidase conjugated rabbit α-mouse IgM or IgG. Ortho-phenylene diamine was added and the reaction was stopped with 4M H_2SO_4. Transmitted light was measured at 490 nm.

3.12 Quantitative RT-PCR

Total RNA was isolated with the RNeasy Plus Mini Kit (Qiagen) and was treated with DNase I (Sigma-Aldrich). cDNA was prepared with the High Capacity cDNA Archive Kit (Applied Biosystems). PCR primers used for real-time quantitative amplification of Glycam1, Madcam1, B3gnt3, Gcnt1, Chst2, Chst4, and Fut7 were described in [61]. PCR primers for Cd34, endomucin, Cd300lg, podocalyxin-like protein, 18S rRNA, and Hprt1 were designed by Primer Express Software (Applied Biosystems). PCRs were run in triplicates using the Power Sybr Green Master Mix (Applied Biosystems) on an ABI 7500 Real Time PCR System

(Applied Biosystems). Standard curves were generated for each transcript, and expression levels were normalized to β-actin; the relative expressions were calculated using β-actin normalized expression levels of wild-type spleens as reference samples.

3.13 Statistical analysis

Normal distributions of means were tested with a one-sample Kolmogorov-Smirnov test. Means were compared with one-way ANOVA, followed by a Bonferroni test. A p value < 0.05 was considered statistically significant. Statistical analyses were performed with SPSS 14.0 software.

4 Results

4.1. Vascular reprogramming of splenic vasculature in Nkx2.3$^{-/-}$ mice

4.1.1. *Lymphocyte composition of the spleen of Nkx2.3 KO mutant mice is similar to that of lymph nodes.*

Earlier studies revealed multiple developmental alteration of various endothelial compartments of the spleen in Nkx2.3$^{-/-}$ mice [17], [25]. However, in spite of the lack of vascular components that may have potential role in the splenic homing of B and T lymphocytes, a significant accumulation of lymphoid cells in the mutant spleen is still preserved, suggesting the presence of tissue structures that are able to mediate lymphoid entry. To define the lymphocyte subpopulations present in the spleen, I used flow cytometry. Interestingly, the distribution of T/B lymphocyte populations in the mutant spleen was more similar to that of lymph nodes (either of wild-type or mutant mice) than to that of the wild-type spleen, with a substantially higher frequency of T lymphocytes (Figure 5.). In addition, lymphocytes present in the mutant spleen had a somewhat higher L-selectin expression, also similar to lymph nodes in this respect.

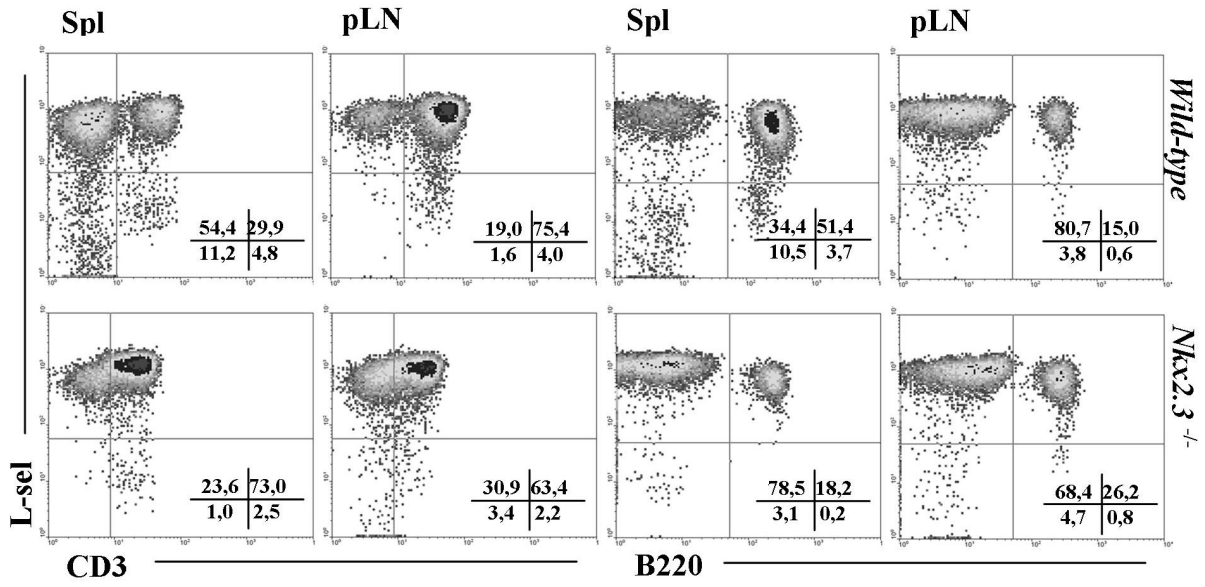

Figure 5. Lymph node – like lymphoid composition of Nkx2.3 KO spleen. Relative abundance of T lymphocytes in the mutant spleen (as assessed with CD3 and B220 labeling) renders its cellular composition similar to either wild-type or Nkx2.3 KO lymph nodes, whereas in wt spleen B lymphocyte dominance ($B220^+$ population) is seen. The altered cellular composition is associated with elevated L-selectin expression, another feature related to lymph node – like lymphocyte accumulation in the mutant spleen.

4.1.2. *Altered expression of marker genes associated with high endothelial venule (HEV) development in the spleen and lymph nodes*

The broad structural alterations of Nkx2.3 mutant spleen [17], [25], [26], the lack of MS and red pulp sinuses together with the lymph node-like accumulation of lymphocytes prompted us to examine which molecules / processes could be responsible for the selective accumulation of these cells. Earlier microarray analysis of the Nkx2.3 mutant spleen suggested that expression of several genes associated with endothelium-mediated tissue-specific homing [62]–[67] was altered (data not shown). In this study, we performed real-time PCR to quantify expression of some of these Nkx2.3 regulated candidate genes in wild-type and mutant spleens as well as in pLN-s and mLN-s. The analysis demonstrated profound reduction of MAdCAM-1 expression in the spleen of the homozygous mutant mouse in agreement with previous reports [25],[27]. Importantly, expression of GlyCAM-1 in the mutant spleen was

dramatically upregulated (~10, 000-fold), whereas transcript levels for other marker genes, such as CD34, endomucin, CD300 Ag-like family member G (Cd300lg, also known as nepmucin), and podocalyxin-like protein, were also increased, although to a lesser extent (between 4- and 16-fold) in comparison with wild-type (Figure 6. a). Particularly, the upregulation of the endothelial marker GlyCAM-1 and the reduction of MAdCAM-1 expression in the mutant spleen appeared more similar to pLN-s than in wild-type spleens. In comparison, the pLN-s from Nkx2.3 deficient mice showed a slightly elevated expression of MAdCAM-1 and an equal expression of GlyCAM-1 compared with wild-type mice, whereas mLN-s had less MAdCAM-1 and a higher level of GlyCAM-1 mRNA expression than wild-type controls. The differences between the expression levels of other core protein genes was less dramatic, although the general tendency was an increased mRNA production for all genes investigated. Pdxl, a lesser investigated PNAd core protein, also showed an increased expression in all lymphoid tissues of Nkx2.3 mutants, whereas its expression in mLN-s and pLN-s of wild-type mice was reduced compared with wild-type spleens.

Both GlyCAM-1 and MAdCAM-1 may serve as backbone proteins for PNAd in a process depending on extensive glycosylation and sulfatation, mediated by the glycosyltransferases B3gnt3 and Gcnt1, the fucosyltransferase Fut7, and the sulfotransferases Chst2 and Chst4, the latter also known as HEC-GlcNAc6ST, respectively [68]. Quantitative RT-PCR (qPCR) analysis for these genes in wild-type and mutant spleens revealed that the majority of these transcripts were upregulated in the Nkx2.3$^{-/-}$ mutant, although to different degrees (Figure 6. b). B3gnt3 glycosyltransferase in Nkx2.3 mutant spleen was expressed at a lower amount compared with wild-type spleen; however, this reduced mRNA transcription was also observed at various degrees in lymph nodes from both mutant and wild-type samples. Gcnt1 glycosyltransferase enzyme mRNA was the only transcript showing differences in expression in lymph nodes between Nkx2.3 mutants and wild-type samples in which, both in pLN-s and mLN-s of Nkx2.3 mutant mice, mRNA of Gcnt1 glycosyltransferase was expressed at a robustly increased amount, similarly to the mutant spleen. Chst4 sulfotransferase mRNA showed a similar degree of increased expression in the mutant spleen as well as in the pLN-s and mLN-s from both mutant and wild-type mice. Taken together, these observations suggest that, in the absence of the transcription factor Nkx2.3, endothelial MAdCAM-1 expression in the spleen is essentially replaced by GlyCAM-1, and the modifying enzymes required to generate functional PNAd are also upregulated. Thus, this pattern of endothelial marker gene expression in mutant spleens is reminiscent of HEVs in pLN-s.

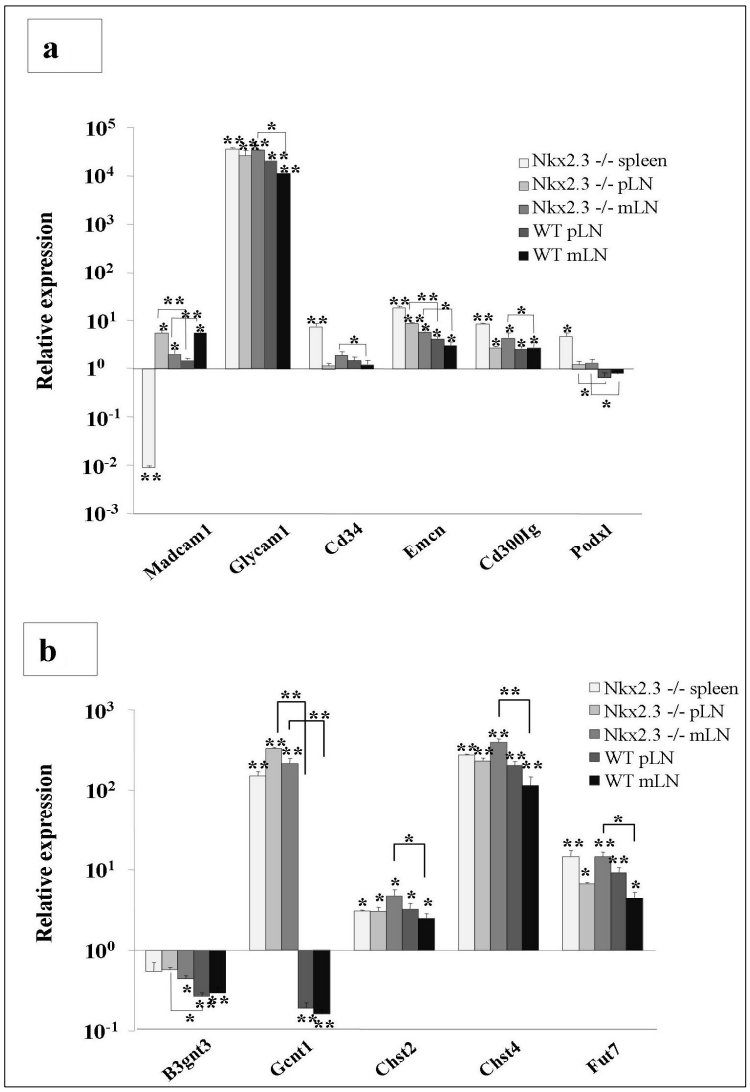

Figure 6. qPCR analysis of mRNAs for PNAd core proteins (a,) and modifying enzymes (b,) in the Nkx2.3 KO and wild-type spleens, pLN-s, and mLN-s. Values in different organs are normalized to the ratio of target mRNA to β-actin in the wt spleen, represented by the line drawn at y = 1, and are expressed on a log scale. Bar diagram shows the mean ± SD of six parallel samples from three mice per organ; *p< 0.05, **p<0.001.

4.1.3. *Ectopic formation of HEV-like vessels in the Nkx2.3$^{-/-}$ mutant spleen*

The pLN-like signature of transcripts for HEV-related genes and the described alterations of the marginal zone and white pulp [16], [17], [25], [27], [69] in the Nkx2.3–deficient spleen prompted us to investigate the vasculature in more detail by using MECA-79 anti-PNAd [70] and anti–MAdCAM-1 mAbs. In contrast to the wild-type spleen, which never

contains PNAd-positive HEVs, in the spleens of young adult Nkx2.3$^{-/-}$ mice, PNAd-positive HEVs in close proximity of B cell-rich foci were prominently present (Figure 7. a). Furthermore, dual immunofluorescence for HEC-GlcNAc6ST sulfotransferase [60] and the PNAd epitope showed coexpression on HEV-like vessels in the mutant spleen, similarly to pLN-s from either wild-type or mutant mice (Figure 7. b). These vessels were lined with plump endothelial cells that express CD31 endothelial marker in which transmigrating lymphocytes could also readily be observed (Figure 7. a).

To test whether the PNAd epitope is accessible for recirculating lymphocytes, MECA-79 mAb against PNAd was administered to Nkx2.3$^{-/-}$ mutants and wild-type mice i.v. We found a strong luminal binding in mutant spleens to a degree similar to pLN-s from either mutant or wild-type mice, demonstrating that this L-selectin ligand is accessible for recirculating lymphocytes in the mutant spleen, similarly to pLN-s (Figure 7. b) whereas wild-type spleens had no discernible reactivity.

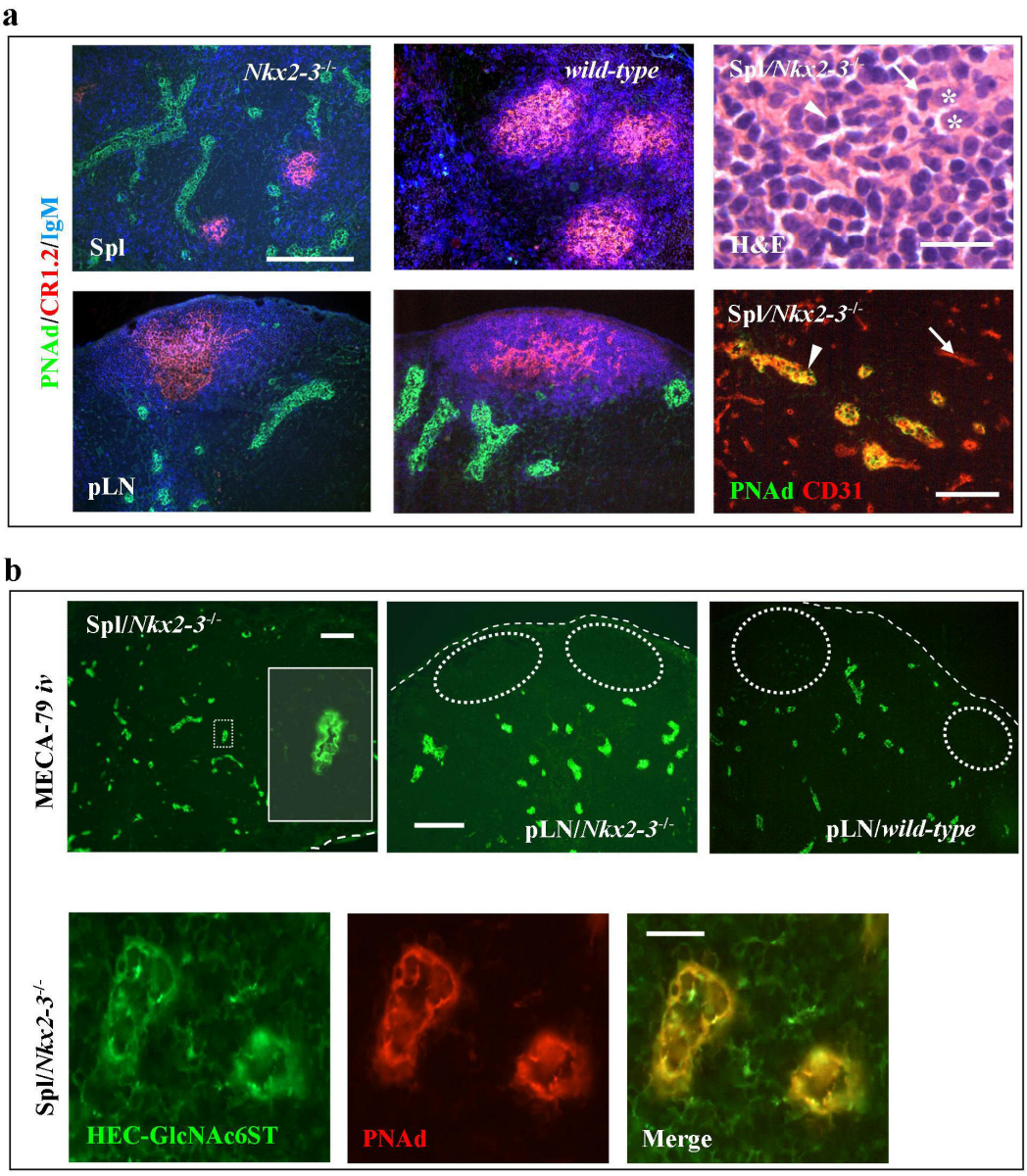

Figure 7. Absence of the Nkx2.3 gene in the BALB/c mouse leads to leukocyte-accessible HEV formation in the spleen. a, Frozen sections of the spleen and pLN-s from mutant and wild-type mice were stained with fluorescence-labeled Abs as indicated. The purple colour represents the merge of complement receptor (CR) expression by FDCs and IgM reactivity of adjacent B cells. Scale bar, 100 μm. H&E staining (upper right) shows plump endothelial cells (asterisks) and lymphocytes either closely associated with (arrowhead) or transmigrating between (arrow) these cells (scale bar, 25 μm). Endothelial cells in the mutant spleen coexpress CD31 and PNAd (lower right). Scale bar, 100 μm. b, The PNAd epitope is detected at the luminal surface of the endothelium in HEVs in the mutant spleen (upper left) and pLN-s from mutant (middle) or wild-type (upper right) mice following i.v. administration of MECA-79 anti-PNAd mAb. Dashed lines represent edges of tissue. Inset, higher magnification of the marked rectangular area in left panel. Ellipses in the pLN sections demarcate follicles. Scale

bar, 100 μm. Lower panels: PNAd positive HEVs strongly coexpress HEC-GlcNAc6ST in the Nkx2.3$^{-/-}$ spleen. Scale bar, 50 μm. The figures are representative from a cohort of three to five mice repeated three times.

4.1.4. *Ectopic HEV-like vessels in Nkx2.3$^{-/-}$ spleen mediate lymphocyte homing in an L-selectin-dependent manner, and express CCL21 arrest chemokine.*

To test whether ectopic HEV-like vessels of Nkx2.3$^{-/-}$ spleen serve as lymphocyte exit ports, CFSE-labeled lymphocytes were i.v transferred into mutant and wild-type mice followed by double fluorescent examination of the animals spleen and pLN. Shortly after injection, labeled lypmhocytes largely accumulated around the MS in wild-type spleen. The accumulation of the lymphocytes in either the mutant spleen or similarly in the pLN-s was less prominent, and lymphocytes were closely associated to the HEV-s in these organs (Figure 8. a). By 12 h, the lymphocytes showed the same degree of tissue dispersion as in peripheral lymph nodes and in the mutant spleen (data not shown).

In pLN-s, binding to HEVs critically requires L-selectin. To determine whether the presence of PNAd^{+} HEVs in the spleen is coupled with an altered dependence on L-selectin during homing, we performed short-term competitive homing experiments in which wild-type lymphocytes were treated with the specific antibody MEL-14 to block L-selectin [71] (Figure 8. b). This mAb prevents the homing of lymphocytes to pLN-s *in vivo* but does not eliminate the cells [72]. Equal numbers of CFSE-labeled lymphocytes treated with MEL-14 mAb and mock-treated biotinylated control cells [61] were then injected into Nkx2.3$^{-/-}$ mutant and wild-type recipients. Thirty minutes after the injection, spleen and pLN cells were isolated and subjected to flow cytometry. We observed that the homing of mock-treated biotinylated lymphocytes in the spleen of Nkx2.3$^{-/-}$ mutants was reduced compared with that in wild-type recipients, but more importantly, the homing of MEL-14 mAb-treated CFSE-labeled cells to the mutant spleen was significantly blocked compared with wild-type recipients. The impaired homing activity of lymphocytes with blocked L-selectin function was indicated by a 3-fold decrease in the CFSE:biotin ratio in the Nkx2.3-deficient spleen but not in the wild-type spleen. The ratio in the mutant spleen was very similar to that in pLN-s of wild-type or mutant mice, suggesting that the ectopic PNAd^{+} HEV-like vessels in the mutant spleen use L-selectin for lymphocyte homing. As expected, blocking L-selectin significantly reduces the ratio of CFSE:biotin-labeled cells in both wild-type and mutant pLN-s, confirming that lymph

nodes use L-selectin–dependent homing mechanism, regardless of the Nkx2.3 genotype. Interestingly, the biodistribution of variously labeled lymphocytes without MEL-14 blockade also revealed a striking parallel between the mutant spleen and pLN-s. The biotinylation of lymphocytes favoured their splenic homing in wild-type mice, whereas in pLN-s, the frequency of CFSE cells was higher, resulting in a CFSE:biotin ratio < 1 in the wild-type spleen, and CFSE:biotin ratio > 1 in pLN-s as well as in the mutant spleens.

After the arrest of lymphocytes in HEV, mediated by PNAd and L-selectin interaction, lymphocyte transmigration is dependent on CCL21 arrest chemokine expressed by the HEV of LNs [73]. To investigate, whether ectopic HEV of the spleen of Nkx2.3-deficient mice express CCL21, double fluorescent labeling was performed with MECA-79 and anti-CCL21 mAb-s (Figure 8. c). While in wild-type spleen, CCL21 labeling was restricted to the fibroreticular network of PALS, in Nkx2.3-deficient spleen CCL21 co-localized with PNAd, similarly to LNs.

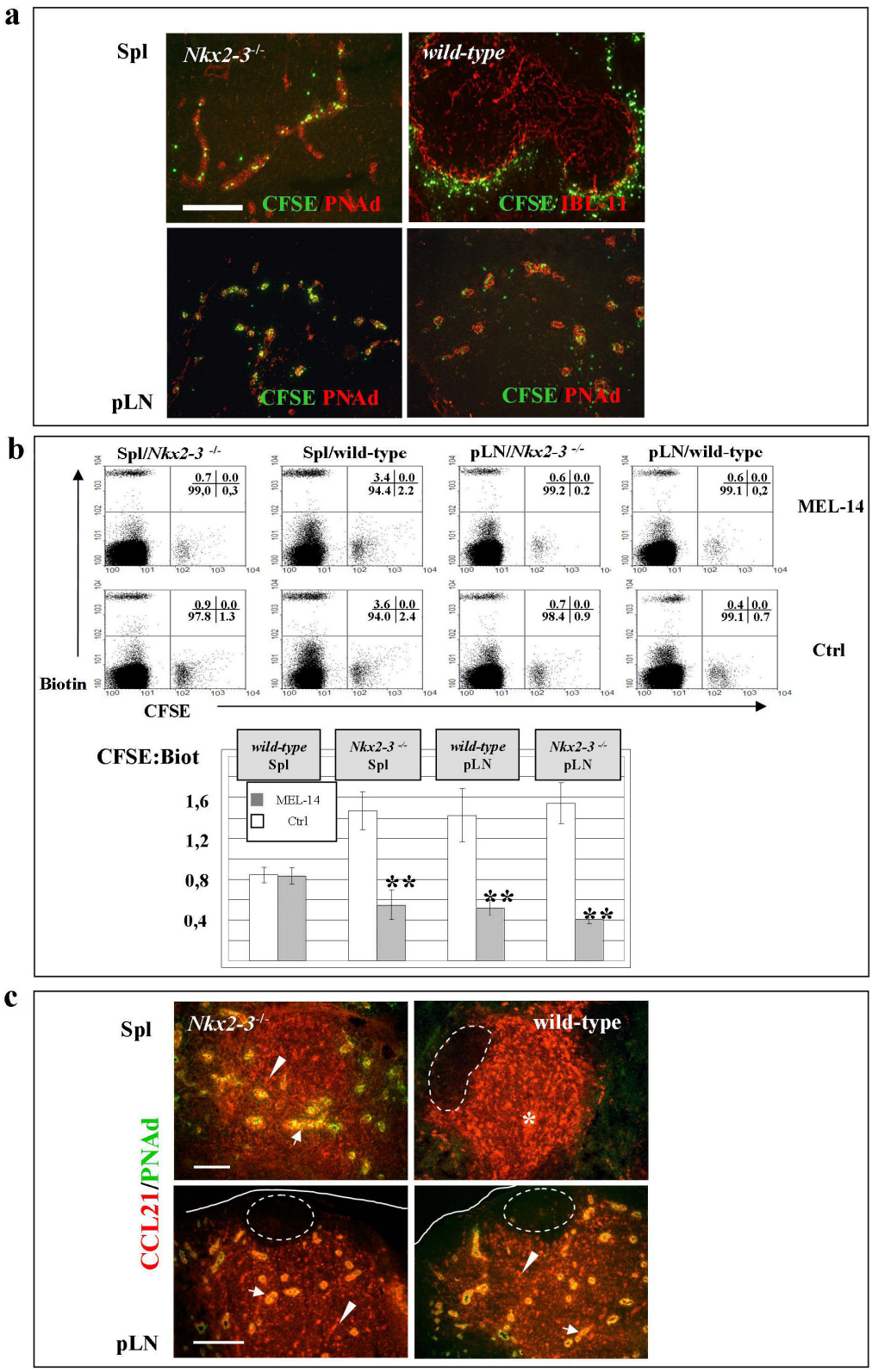

Figure 8. HEVs in Nkx2.3$^{-/-}$ mice function as L-selectin–dependent exit ports to the spleen and express CCL21. a, CFSE-labeled lymphocytes (green) are localized to HEVs identified with MECA-79 anti-PNAd mAb (red) in the Nkx2.3$^{-/-}$ spleen (left) and pLN 30 min after i.v. injection. In the wild-type spleen (right), the lymphocytes are associated with the

marginal zone visualized by IBL-11 mAb. Scale bar, 200 μm; the results are representative for three independent experiments with at least three mice each. b, MEL-14 mAb against L-selectin reduces short-term homing to the spleen and pLN in Nkx2.3$^{-/-}$ mice. CFSE-labeled cells were treated with MEL-14 mAb or control mAb and injected together with biotinylated cells into wild-type or Nkx2.3$^{-/-}$ mutant recipients. Numbers indicate the percentages of cells in the four quadrants. The lower diagram summarizes the results of three independent experiments performed with three to five mice for each genotype. The percentage data of retrieved cells were corrected by the ratio of CFSE:biotinylated cell percentages in the preinjection mixture. Shaded bars, MEL-14 mAb; open bars, control mAb; **$p < 0.001$. c, PNAd^{+} HEV-s express CCL21 in Nkx2.3$^{-/-}$ spleen (upper left, arrows) as well as in LNs (lower panels, arrows), together with fibroblast of the T-cell zone (arrowheads). On the other hand, CCL21 labeling is mostly restricted to the fibroreticular cells of the PALS around the central arteliole (asterisk) in wild-type spleen, without noticeable MECA-79 reactivity; circles represent follicles, scale bar 200 μm.

4.2. *In situ* CFSE labeling reveals mutual kinetic exchange of peritoneal B-1 cells with B-1 cells of other niches

Along with characterizing the extent of stromal changes of the spleen in Nkx2.3$^{-/-}$ mutant mice, I also sought to examine the effect of this mutation on the homeostatic changes of B-1a cells, a population of which the maintenance is dependent on the spleen [30], [48], [49]. Examining B-1 cell homeostasis under distinct conditions is largely based on the measurement of the ratio and/or absolute number of peritoneal B-1a cells, as an easily accessible source of this population. However, it is unknown to what extent peritoneal B-1a cells represent the complete B-1a pool of the immune system, and whether there is a mutual exchange of B-1a cells among distinct compartments (e.g. peritoneal, pleural cavity and spleen).

Studies addressing the *in vivo* behaviour of B-1 cells usually rely on adoptive cell transfer of genotype-marked cells (based on CD45 or MHC allotype, or green fluorescent protein expression) or cells labeled *ex vivo*, thus altering the cellular composition of recipients. In these approaches, both the *ex vivo* manipulation of donor lymphocytes prior to transfer and the administration of excess lymphocytes may significantly influence subsequent retention and departure of both the resident and inoculated cells, thereby affecting the interpretation of results. Therefore, procedures avoiding these possible influences are necessary for the follow-up of these cells under physiological conditions. Another approach – without the requirement of excessive cell transfer – is establishing parabiotic models, where mutual exchange of cells has been revealed; however, the exact source of the cells could not be determined (i.e. whether cells of peritoneal origin home to the pleural cavities as well, or only to the peritoneal cavity of the parabiotic partner) [74].

To address the issue of peritoneal lymphocyte homeostasis in steady-state conditions without cell transfer, we developed a novel assay for their long-term follow-up using CFSE via *in situ* administration. Several properties of CFSE make it a versatile tracing compound. CFSE is trapped in the cells after acetate groups are cleaved off by intracellular esterases, and the resulting product stably binds to the free amino groups of the intracellular proteins through its succinimidyl part without cytotoxic effects. Thus CFSE is an ideal tracing compound in pulse-labeling/cell tracing experiments, even when administered *in vivo* [75].

4.2.1 *Efficient and selective labeling of peritoneal leukocytes in vivo*

Previous studies revealed that intravenous administration of CFSE could achieve stable fluorescent labeling of leukocytes in a heterogeneous pattern, despite the presence of esterases in serum [76]. This raised the possibility that the anatomically isolated peritoneal cells can also be selectively labeled with the same compound *in situ*. We found that a single intraperitoneal injection of CFSE at an optimized dose and volume was sufficient to label the overwhelming majority of cells residing there. Flow cytometric analyses performed shortly after the labeling (0.5 h) revealed that both peritoneal lymphoid and myeloid cells were labeled. Subsequently, we confirmed that the tracer did not reach leukocytes in other lymphoid organs, including blood, spleen, peripheral and mesenteric lymph nodes and pleural cavity (Figure 9. a). On the other hand, the serosal lining of intestines and the splenic capsule were also labeled upon CFSE injection (Figure 9. b), without reaching deeper regions of the tissues.

We also compared the efficiency of *in situ* labeling to that of adoptive transfer of *ex vivo*-labeled cells. Despite the intraperitoneal injection of a large number of CFSE-labeled peritoneal cells (corresponding to three donors/single recipient cell load), we found that the frequency of $CFSE^+$ lymphocytes within the peritoneal lymphoid compartment was 30%, 6 h after adoptive cell transfer. In contrast, 85% of lymphocytes were $CFSE^+$ at the same period after *in situ* labeling (Figure 9. c). This high labeling efficiency confers a considerably more representative labeling of peritoneal lymphocyte upon intraperitoneal CFSE administration. Although the *in situ* labeling showed a heterogeneous pattern, it was nevertheless consistently reproducible and permitted a clear separation from the control cells with background autofluorescence.

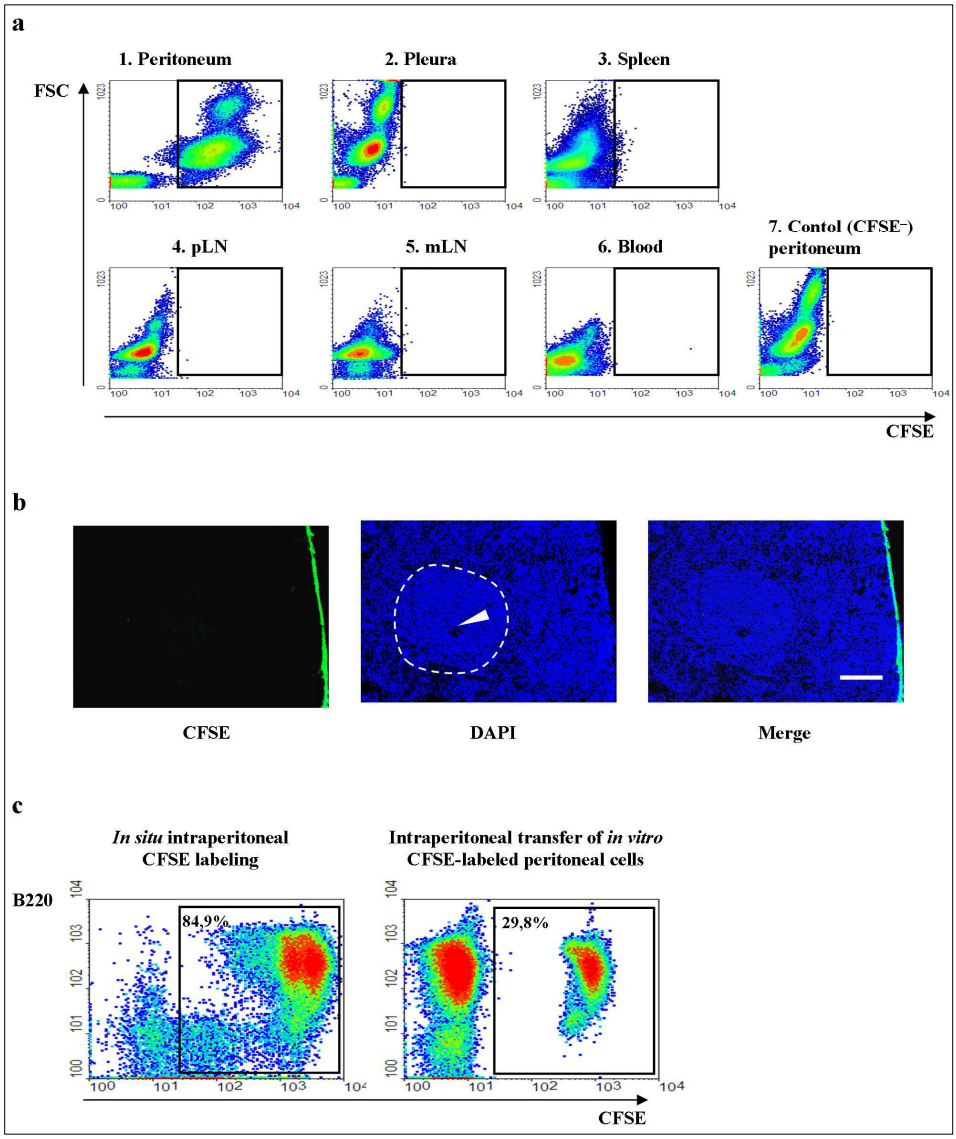

Figure 9. ***In situ*** **CFSE delivery efficiently labels peritoneal leukocytes. a,** CFSE versus forward scatter plot of the cells from various lymphoid organs as indicated at the top 30 min after intraperitoneal CFSE injection. Autofluorescence without CFSE labeling ($CFSE^-$ mouse) is also shown. b, Fluorescence of the spleen 30 min after peritoneal CFSE labeling. CFSE fluorescence labeling (left) is confined to the mesothelial lining of the spleen upon *in situ* CFSE administration, without expanding into the deeper layers (DAPI nuclear staining, middle; merge, right). Dotted line encircles the white pulp, arrowhead points to central arteriole (scale bar, 200 μm). c, Comparison of *in situ* intraperitoneal CFSE labeling with intraperitoneal adoptive transfer of *in vitro* CFSE-labeled peritoneal cells. Mice were injected either with CFSE solution (left) or with 5 x 10^6 *in vitro* CFSE-labeled peritoneal cells (right). CFSE labeling of peritoneal lymphocytes was assessed 6 h after injections, plotted against B220 expression. Numbers in the regions represent percentage ratio of $CFSE^+$ cells within the lymphoid compartment. Panels show representative results of at least three independent experiments.

4.2.2 *Intraperitoneal administration of CFSE reveals different exchange kinetics of peritoneal leukocyte sub-populations under steady-state conditions*

Next, I investigated whether various peritoneal leukocyte subsets show different tissue replacement kinetics by determining the proportion of $CFSE^+$ cells over time. Peritoneal lymphocyte sub-populations (B-1, B-2 and T) were identified based on their B220, Mac-1 and CD5 expression, respectively, and the percentage of $CFSE^+$ cells was examined within these populations from 6 h to 4 weeks after *in situ* CFSE labeling. Analysis performed at 6 h post-injection showed differential dye retention and exchange kinetics between myeloid cells and lymphocyte subsets. I found that a substantial part of Mac-1^+ myeloid cells were either $CFSE^-$ (indicating their recent entry into the peritoneal cavity subsequent to the injection) or $CFSE^{dim}$, as a result of faster release of intracellular protein–CFSE conjugates (Figure 10. a). Interestingly, the injection of CFSE or the solvent alone was sufficient to induce a transient influx of myeloid cells into the peritoneal cavity within 6 h. The resulting myeloid excess elapsed in 1 week (Figure 10. a). Shortly after injection, T cells contained the highest proportion of $CFSE^-$ lymphocyte subset. Six hours after *in situ* CFSE labeling, 50% of the peritoneal T cells were $CFSE^+$ on average, reflecting an exchange of 50% of peritoneal T lymphocytes to extraperitoneal T cells during this period (Figure 10. b and c). After 1 week, the frequency of $CFSE^+$ T cells remained constant at 2 to 5% of the total peritoneal T-cell pool. For B cells, this event was substantially slower and showed a strong correlation with the B-1/B-2 phenotype of B cells. Six hours after the labeling, a striking difference for CFSE retention was noted in B-1 and B-2 cells. B-1 cells contained a rather homogeneous population with intense fluorescence ($CFSE^{hi}$) with only a small fraction of lesser CFSE fluorescence, whereas the CFSE profile of B-2 cells was more heterogeneous, containing a substantial subset with reduced CFSE labeling ($CFSE^{dim}$), while a small fraction of cells was already exchanged for extraperitoneal cells ($CFSE^{neg}$; Figure 10. b). Subsequent follow-up revealed that the 50% exchange ratio was achieved over 2 days for B-2 and 2 weeks for B-1 cells after CFSE labeling, respectively (Figure 10. c). Within the B-1 population, no significant differences were observed between the exchange kinetics of B-1a and B-1b cells during this period (data not shown); thus, B-1a and B-1b cells were evaluated as a single, common B-1 population hereafter in this study. The ratio of $CFSE^+$ B-1 cells is stabilized after 2 weeks, at 45 to 50% of total B-1 cells with detectable CFSE label, and it remains stable

for at least two more weeks. In contrast, the decrease of $CFSE^+$ ratios of B-2 cells continued during the 4-week interval. Importantly, decrease in the ratio of CFSE-labeled cells was not due to an anti-fluorescein response because no fluorescein-specific antibodies could be detected in the serum of mice between 2 and 4 weeks after CFSE injection (data not shown). These results indicate that, among peritoneal lymphocytes, under steady-state conditions, T cells have the fastest exchange rate. B-2 cells are replaced at a slower pace. B-1 cells reside for the longest period in the peritoneal cavity and are exchanged for extraperitoneal B-1 (CFSE-negative) cells at the slowest kinetics but remain stable after reaching equilibrium.

To determine the re-distribution of *in situ*-labeled lymphocytes after their departure from the peritoneal cavity, we analyzed peripheral lymphoid tissues and the blood for tracing CFSE-labeled cells. We found that a small, but a detectable amount of B cells appeared in the peripheral blood and in the spleen 24–48 h after labeling, respectively (Figure 10. d). Lymph nodes remained mostly devoid of $CFSE^+$ cells throughout the period of observation (data not shown).

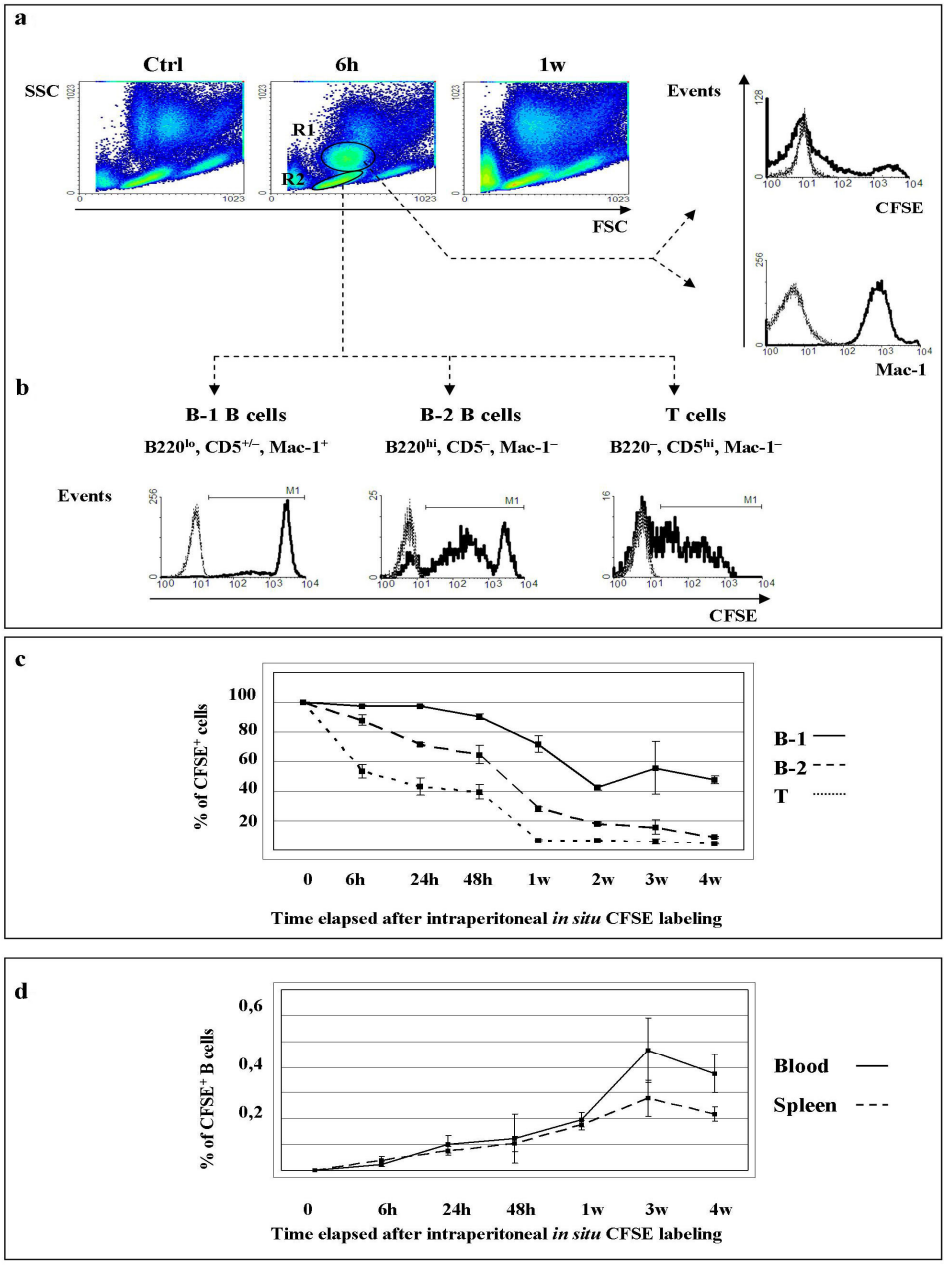

Figure 10. Intraperitoneal CFSE labeling reveals differential exchange kinetics of peritoneal leukocyte subsets and permits extraperitoneal tracing of *in situ*-labeled peritoneal B cells. a, Compared with untreated controls, intraperitoneal injection induces early (6 h) myeloid influx leading to reduced $CFSE^+$ fraction (upper histogram overlay; $CFSE^+$ cells, solid line; autofluorescence of untreated sample, dashed line) from extraperitoneal compartments, which is resolved in 1 week, resulting in similar peritoneal cells composition to untreated sample (forward scatter [FSC]/side scatter [SSC] density plot, right). These myeloid cells (in R1 gate defined by size and granularity) express Mac-1 antigen (solid line in lower histogram overlay; dashed line, isotype control). b, CFSE profile of peritoneal lymphoid subsets (defined by their B220, Mac-1 and CD5 expression) 6 h after *in situ* labeling. In the histograms, dashed lines represent negative staining control and the M1

corresponds to $CFSE^+$ cells, respectively. c, Differential decrease in the ratio of $CFSE^+$ cells from 6 h to 4 weeks after *in situ* labeling reveals different exchange kinetics of peritoneal B-1, B-2 and T cells. Data represent mean + standard error of the mean (SEM). d, Detectable proportion of $CFSE^+$ B cells appears in the blood and spleen already at 24 and 48 h after labeling, respectively. The 0.1% frequency of $CFSE^+$ cells was set as detection level above background (n = 6).

4.2.3 *LPS induced egress and division of peritoneal B cells is associated with enhanced preferential homing of B-1 cells in the pleural cavity*

In vitro and *in vivo* data indicate that stimulation of B cells through TLR4 has a complex effect on B cells including enhanced proliferation and rapid egress of B-1 cells from the peritoneal cavity [75], [76], [77]. Therefore, we next examined the effect of a single intraperitoneal LPS injection on peritoneal B-cell homeostasis delivered 2 h after *in situ* CFSE labeling, when the overwhelming majority of B-2 and B-1 cells is $CFSE^+$. Changes both in the proportion of $CFSE^+$ cells and in the CFSE intensity were examined from 6 h to 1 week after LPS administration. As an initial effect of TLR4 stimulation, LPS induced a dramatic egress of both peritoneal B-2 and B-1 cells 24 h after stimulation, reflected by an 50 and 40% decrease in the absolute number of both subsets, respectively (Figure 11. a). Enhanced exit of peritoneal B cells is also supported by the appearance of a significantly higher proportion of $CFSE^+$ B lymphocytes in the blood and in the spleen 48 h and 1 week after LPS injection, respectively (data not shown). At 1 week, the absolute number of peritoneal B-1 cells returned to normal level, whereas the number of B-2 cells was 2-fold higher than in control animals (Figure 11. a). Restoration of the B-cell compartment by this time is attributed both to LPS-induced proliferation and to enhanced homeostatic immigration of B cells from extraperitoneal niches following LPS-induced egress. The extent of LPS induced proliferation of both B-1 and B-2 cells could be determined by comparing the $CFSE^{dim}/CFSE^{hi}$ (i.e. the already divided/not divided) fraction of the respective populations with, or without LPS treatment (Figure 11. b). According to these both B-2 and B-1 cells proliferate considerably upon *in situ* LPS stimulation. The enhanced entry of extraperitoneal lymphocytes into the peritoneal cavity upon LPS treatment is reflected by the lower proportion of both $CFSE^+$ B-2 and B-1 cells at 1 week in the peritoneum of LPS-treated mice compared with control animals (Figure 11. c).

In addition to peritoneal accumulation, B-1 cells are also present in the pleural cavity [78],[79], although the relationship to their peritoneal counterparts has remained elusive. B-1 cells in long-term parabiosis experiments using alloantigen detection showed substantial homing to both peritoneal and pleuropericardial cavities [74]. In these latter studies, however, the anatomical (pleural or peritoneal) source of these cells could not be defined. Therefore, we tested whether following their *in situ* labeling, peritoneal B-1 cells would relocate in the pleural cavity and how their inter-cavity distribution can be modulated by exposure to LPS. Our initial studies showed that the diaphragm efficiently prevented the pleural uptake of intraperitoneally administered CFSE (see Figure 9. a, b). The frequency of both $CFSE^+$ B-1 and $CFSE^+$ B-2 cells within the pleural cavity rose gradually after labeling, although with different kinetics. The frequency of $CFSE^+$ B-2 cells reached its peak at 1-week post-labeling at 0.8%, whereas the $CFSE^+$ B-1 cells continued to increase up to the third week when they reached a frequency of 7% (Figure 12. a). This pleural accumulation of $CFSE^+$ B-1 cells was 3-fold accelerated by LPS stimulation shortly after the *in situ* labeling by the end of the first week, while the accumulation of $CFSE^+$ B-2 cells did not change significantly (Figure 12. b, c). These data indicate that although both peritoneal B-1 and B-2 cells have the preference for pleural migration, LPS promotes an increased activity only for the B-1 cells to target pleural cavity. The increased pleural entry of $CFSE^+$ B-1 cells was detectable as early as 1 day after LPS treatment, which corresponds to the decline of $CFSE^+$ B-1 cells in the peritoneum. Furthermore, changes in CFSE pattern upon LPS-induced B-cell division was also reflected by $CFSE^+$ B cells residing in the pleural cavity 1 week after LPS stimulation (compare Figure 11. b and Figure 12. c), showing an increased frequency of B-1 cells with reduced CFSE retention.

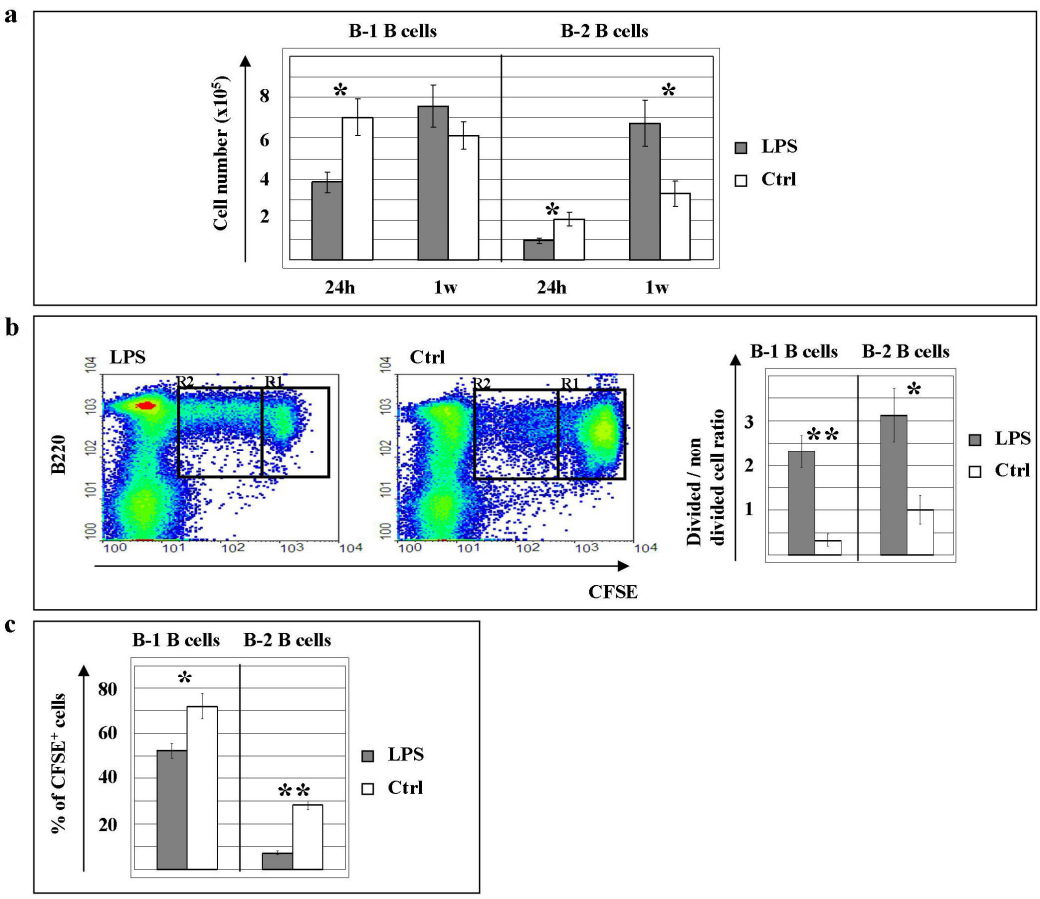

Figure 11. TLR4 stimulation of both peritoneal B-2 and B-1 B cells induce their enhanced peritoneal egress and proliferation. Two hours after *in situ* CFSE labeling, peritoneal B cells were stimulated with LPS as described in Methods. a, The absolute number of B-2 and B-1 cells decreases 24 h after LPS stimulation and is restored 1 week later. b, LPS-induced proliferation of peritoneal B cells is revealed by division-linked decrease in CFSE intensity at 1 week after LPS administration. Flow cytometric plots show analysis gates for B cells (B220) without division (R1: $CFSE^{hi}$) or cells that have undergone division (R2: $CFSE^{dim}$). The bar diagrams illustrate the R2/R1 ratio of B-1 or B-2 cells identified by their B220 and Mac-1 profile. c, In LPS-treated mice, the $CFSE^{+}/CFSE^{-}$ ratios within both B-2 and B-1 subsets are significantly lower in the peritoneal lavage 1 week after stimulation, due to enhanced homeostatic immigration of B cells from extraperitoneal sites following LPS-induced B-cell egress (n = 8). Data in the diagrams represent mean ± SEM. * and ** indicate P values of <0.05 and <0.005, respectively.

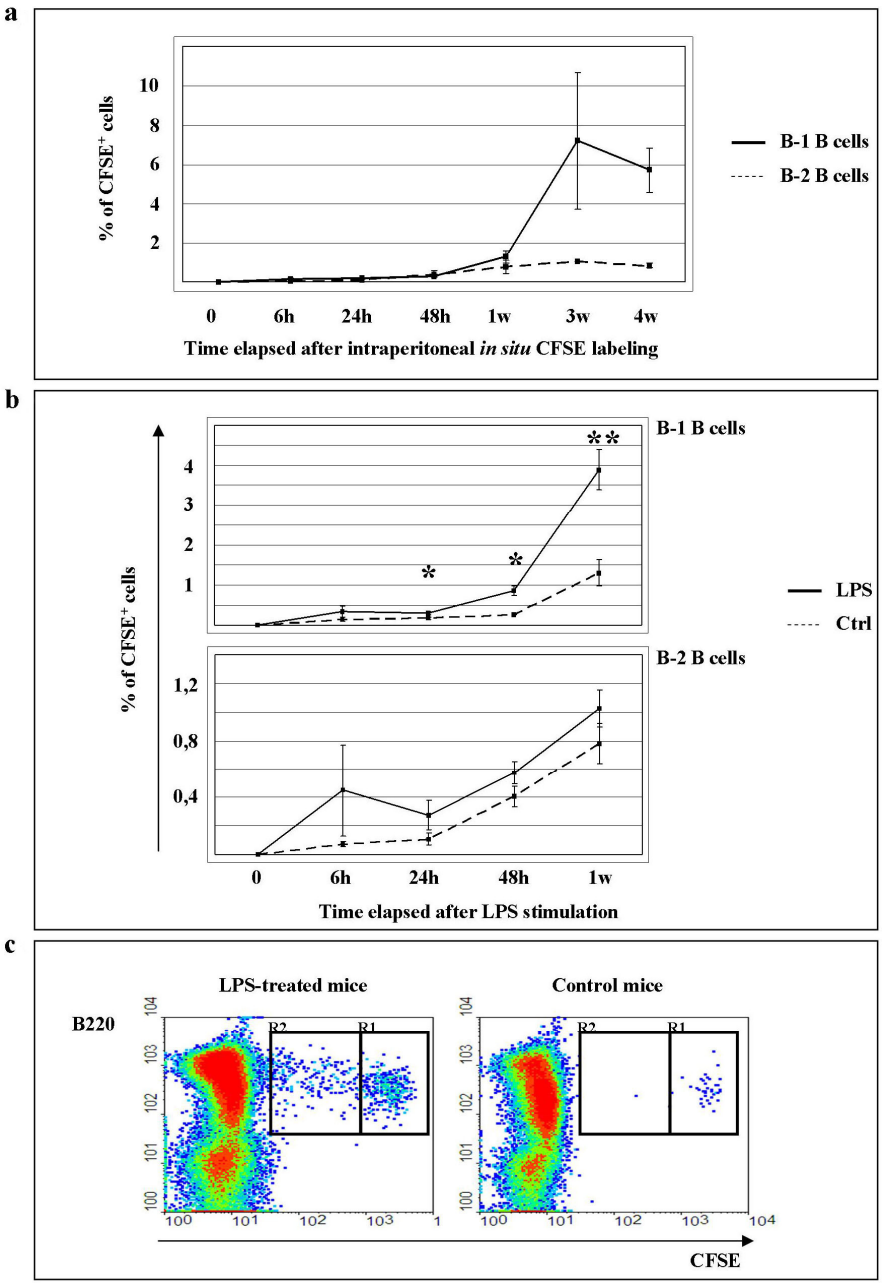

Figure 12. LPS stimulation selectively enhances the preferential homing of B-1 cells to serosal cavities. Pleural B-1 and B-2 subsets were identified similarly to peritoneal counterparts. Proportion of $CFSE^+$ cells was determined within each subset at different periods (horizontal axis) after intraperitoneal CFSE labeling. a, Both peritoneal B-1 and B-2 cells preferentially accumulate in the pleural cavity, with a higher serosal homing capacity of B-1 cells. b, Intraperitoneal LPS injection enhances pleural translocation of B-1 cells, without affecting the pleural homing of B-2 cells. c, CFSE pattern of pleural B cells (B220) following inter-cavity translocation is similar to those remaining in the peritoneum at 1 week after LPS stimulation (left), with an increased proportion of proliferating cells (R2), whereas control lavage contains mostly $CFSE^+$ non-dividing cells (right, R1). Figure shows representative density plots of pleural lymphocytes. Data were achieved from at least four mice per group in

two independent experiments showing the same results. Data in the diagrams represent mean ± SEM. * and ** indicate P values of <0.05 and <0.005, respectively.

Taken together, these results suggest that the *in situ* intraperitoneal CFSE labeling technique is a reliable mean for representative and selective labeling of peritoneal lymphocytes. With this technique we described, on a so far unexamined time-scale (from 6h – to 4 weeks) the exchange kinetics of distinct peritoneal lymphocyte with extraperitoneal sites, with special emphasis on that of B-1 cells. Furthermore, we proved for the first time that the peritoneal and pleural B-1 cell compartments are joined by dynamic exchange between them either under steady state or after LPS stimulation. Thus the easily accessible peritoneal B-1 cell pool may serve as an ideal indicator population of the complete B-1a cell pool of the immune system.

4.3. Homeostasis of B-1a cells in Nkx2.3$^{-/-}$ mutant mice

Extensive studies have shown that the spleen plays an indispensable role in the homeostasis of B-1a cells [30], [48], [49]. However the exact nature and origin of the survival / proliferative signal delivered by the spleen is not known yet. Using mutant mouse models with distinct splenic phenotype may help us understand to what extent distinct tissue components are involved in the B-1a homeostasis and the mechanism the spleen plays in B-1a cell maintenance and function. Accordingly, in this study I made use of the Nkx2.3$^{-/-}$ mutant mouse model of which the splenic phenotype is well established, comprising a profound defect of red pulp and marginal zone architecture [17], [25], the two tissue compartments unique for the spleen. Thus, in addition to the effect of complete lack of spleen, the near-selective absence of red pulp in this mutation may further define the splenic tissue compartment that exerts regulatory role on the maintenance of B-1 B cells. Furthermore, in this mutation the B-1a cell homeostasis has not been examined yet.

Distinct peritoneal lymphocyte populations can be easily distinguished based on their B220, Mac-1 and CD5 expression. Accordingly, within the B-lymphocyte population (B220$^+$ lymphocytes) CD5 and Mac-1 expression defines 3 populations: CD5$^+$ B lymphocytes are B-1a cells, Mac-1$^+$ CD5$^-$ cells represent B-1b lymphocytes, and Mac-1$^-$ CD5$^-$ cells are conventional (B-2) lymphocytes of the peritoneal cavity[37]. Recently B-1a cell population was further divided according to its Mac-1 expression: Mac-1$^+$ CD5$^+$ cells were designated as

B-1a cells, and a minor Mac-1$^-$ CD5$^+$ population was referred to as B-1c cells (Figure 14. a) [80]. According to phenotypic and functional studies, B-1c cells are similar to B-1a cells rather than being B-2 lymphocytes with altered phenotype, and during cell transfer experiments they can readily replace B-1c as well as B-1a cells [51]

4.3.1 *Peritoneal B-cell subsets of identical phenotype are formed in Nkx2.3$^{-/-}$ and BALB/c mice.*

It is well established that the spleen plays an important role in the terminal differentiation stage of naïve conventional B lymphocytes during which several phenotypic changes occur [81]. Furthermore, under certain conditions, CD5 expression can be achieved on B-2 lymphocytes as well [82]. Therefore it is imperative to ensure that in Nkx2.3$^{-/-}$ mutants peritoneal CD5$^+$ B lymphocytes are indeed B-1c and B-1a cells, rather then B-2 cells with altered phenotype caused by a yet unidentified effect due to the structural alterations of spleen in these mice. Therefore, before embarking into detailed examination of the homeostasis of CD5$^+$ B cells in Nkx2.3 KO mice, the nature of these cells were examined.

To address this issue a panel of a cell surface marker specific monoclonal antibodies was used along with B220, Mac-1 and CD5 labeling, and 4-colour flow cytometry of peritoneal lymphocytes of Nkx2.3$^{-/-}$ mutants and wild-type mice was performed (Figure 13.), [83], [84]. Distinct lymphocyte populations were distinguished as described in the introduction of this section, and cell surface marker expression of B-cell subsets was compared. In accordance with earlier reports [80], and similarly to wild-type mice, peritoneal Nkx2.3$^{-/-}$ B-1 cells (B-1b as well as CD5$^+$ cells) had IgM^{hi} IgD^{lo} phenotype. CD5$^+$ B cells expressed significantly higher level of CD43 than B-1b cells, whereas B-2 cells were CD43$^-$. Furthermore, in contrast to B-2 lymphocytes expressing CD23 and having CD21^{dim} phenotype, all of the B-1 cell populations were CD23$^-$ and CD21$^-$. This phenotypic pattern was consistent in the case of the respective B-cell populations either in Nkx2.3$^{-/-}$ mutant and wild-type mice, indicating that the distinct peritoneal B-cell subsets in mutant animals mutually correspond to the respective populations in normal mice.

Importantly, according to their CD23 expression in mutant mice, peritoneal B-2 lymphocyte population was split into a CD23$^-$ and a CD23$^+$ population of nearly equal size (Figure 13. see CD23 panel), whereas this population homogeneously expressed CD23 in wild-type mice [81]. After leaving the bone marrow, naïve B-2 lymphocytes go through a

final developmental stage, while CD23 expression is acquired. Accumulation of a significant proportion of $CD23^-$ B-2 cells in an extrasplenic site (in this case the peritoneal cavity) may also implicate that structural changes in the spleen of $Nkx2.3^{-/-}$ mice alter its function in peripheral lymphocyte homeostasis.

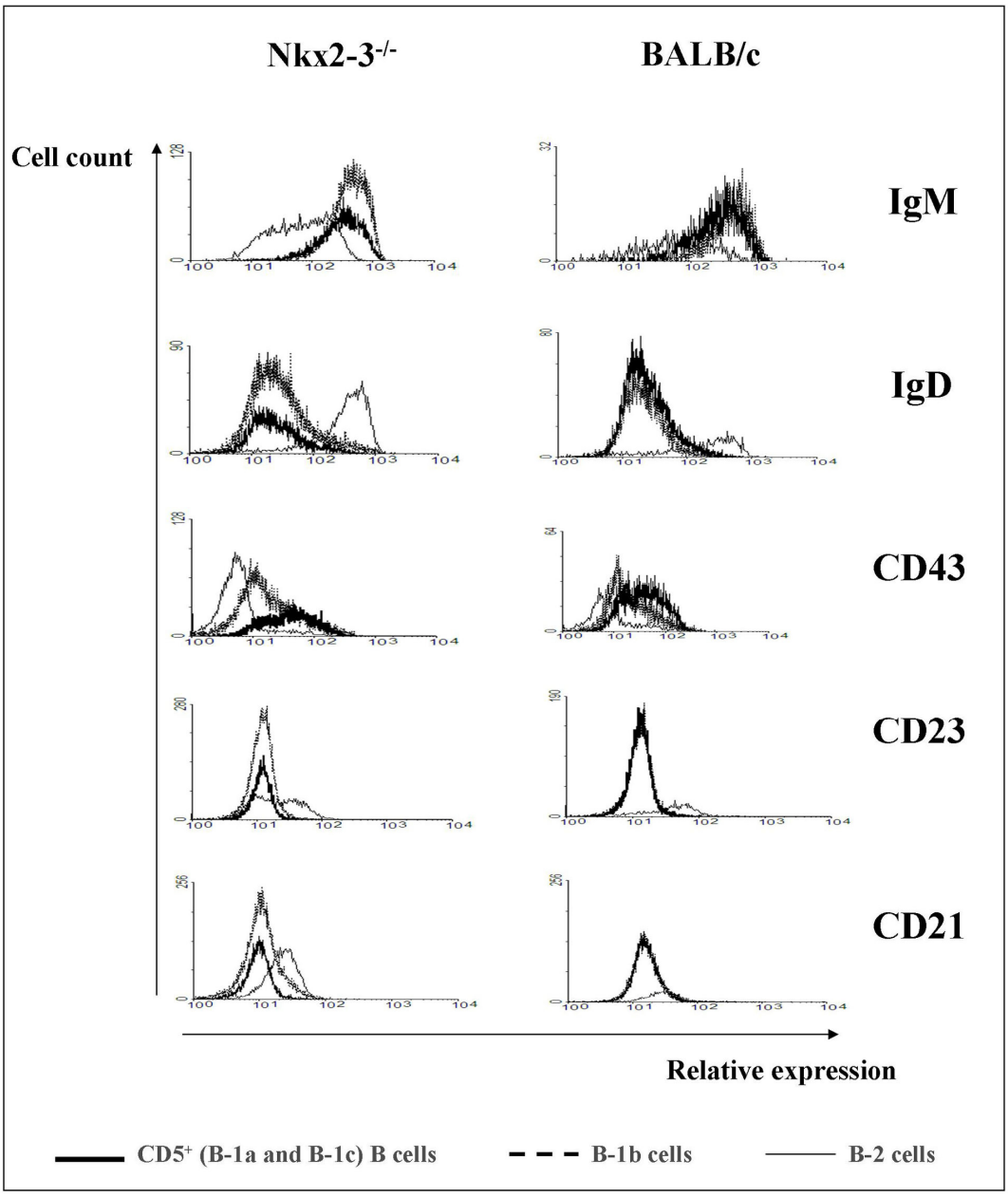

Figure 13. Phenotypic characterization of peritoneal B-cell subsets in $Nkx2.3^{-/-}$ mice. Four colour-staining (B220, Mac-1, CD5, and the respective markers) was performed on pooled peritoneal lavage cells of four 1 month old $Nkx2.3^{-/-}$ and four age-matched BALB/c mice. Cells were analyzed with flow cytometer. Based on a panel of five cell surface markers (IgM, IgD, CD43, CD23, CD21) the phenotype of distinct peritoneal B-lymphocyte subsets was established. Essentially, the corresponding subsets had identical phenotype in mutant and

wild-type mice, with the only exception of CD23, where the appearance of a prominent $CD23^{neg}$ B-2 lymphocyte population may indicate the altered function of the spleen in B-2 lymphocyte maturation of $Nkx2.3^{-/-}$ mutant mice.

4.3.2 *The ratio of peritoneal $CD5^+$ B cells of $Nkx2.3^{-/-}$ mutant mice shows an age-dependent progressive decrease*

To address the peritoneal $CD5^+$ B-cell homeostasis in $Nkx2.3^{-/-}$ mice, peritoneal cell composition of the mutants of various ages were examined with flow cytometry, and compared to age-matched wt mice. The gating scheme used for this examination is shown in Figure 14. a. As a result of the examination, an age dependent decrease in the ratio of $CD5^+$ peritoneal B cells could be seen, with an initial decrease more prominent in the B-1c population, followed by an enhanced decrease in that of B-1a cells (Figure 14. b). Even in young (1 month old) mice, the B-1c, B-1a and – accordingly – the total $CD5^+$ B lymphocyte ratio was markedly lower in mutants than in wild-type animals, with a 50% reduction in B-1c and a 25% reduction in B-1a cells. By 2 month of age, the B-1c cell ratio further decreased to around 21% of that in normal mice. On the other hand between 2 and 4 month of age the decrease in B-1a cell ratio accelerated and, by 4 month, B-1a ratio reached around 30% in mutants of that in wt animals, while the B-1c ratio did not show further significant decrease during this period.

Consistently with and similarly to earlier findings in LTα mutant mouse model, an increase in B-1b cell ratio in young (up to 2 month old) $Nkx2.3^{-/-}$ mutants was found compared to wild-type animals [85]. The initial increase in the ratio of this population may have partially contributed to the initial decrease in the $CD5^+$ B-cell ratio. However, we consider that the changes in the ratio of peritoneal $CD5^+$ B lymphocytes in $Nkx2.3^{-/-}$ mutants is not merely a virtual change caused by the increase in B-1b ratio, but reflects a real homeostatic defect of these cells, as in old (4 month old) mice, both $CD5^+$ populations (B-1c and B-1a) are severely decreased with no other peritoneal B-cell subset alterations compared to normal mice. Similar kinetics was observed concerning changes in the frequency of pleural B-lymphocyte subsets (data not shown).

Throughout our examination, the ratio of peritoneal B-2 lymphocytes was not significantly altered in $Nkx2.3^{-/-}$ mice.

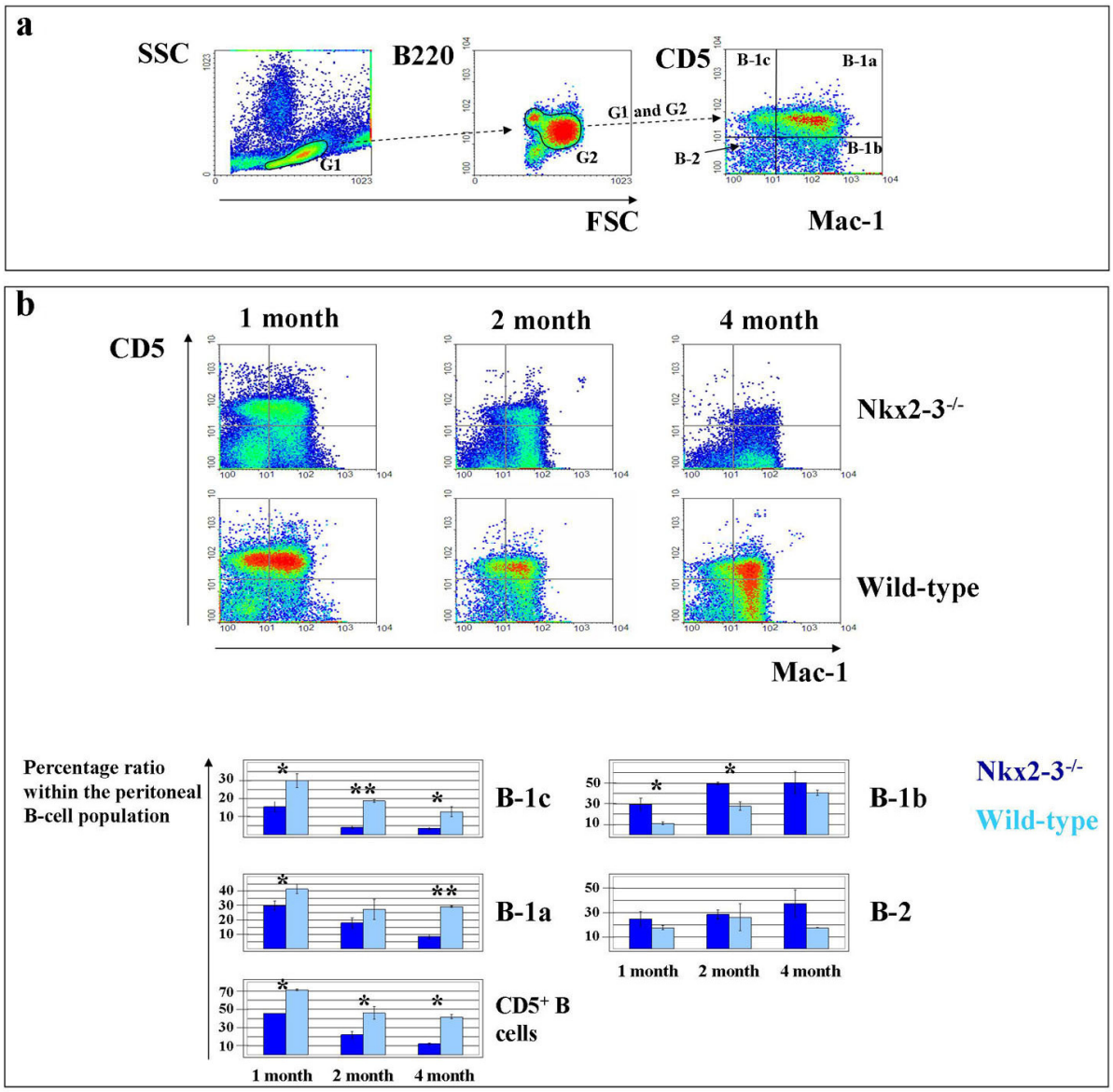

Figure 14. Age-related decrease in the peritoneal CD5$^+$ B-lymphocyte ratio of Nkx2.3$^{-/-}$ mice. a, Peritoneal B cells were identified based on their physical parameters (G1 gate based on FSC, SSC) and B220 (G2 gate) expression. Distinct B-cell subsets were resolved according to their Mac-1 and CD5 expression. b, Three colour-staining (B220, Mac-1 and CD5) of peritoneal lavage cells from Nkx2.3$^{-/-}$ mice at different ages (n=4 per group) was performed. Age-matched BALB/c mice were used as controls. Peritoneal B lymphocytes subsets were identified as described above. Representative density plots are shown. Histograms represent the mean percentage ratio of the respective B-lymphocyte subsets either in mutant of wild-type mice of different age. Error bar = SEM, * p<0,05.

4.3.3 *Progressive decrease in the serum level of natural antibodies of distinct specificities in Nkx2.3$^{-/-}$ mice*

B-1a lymphocytes have been shown to be responsible for the production of natural antibodies of IgM isotype, which provide an early, innate-like protection against invading bacteria and viruses [46], [86], [87], [88]. These antibodies have low affinity towards their antigens and have broad reactivity to conserved antigens on the surface of distinct pathogens with repeated elements (e.g. pneumococcus polysaccharide). B-1a cells do not spontaneously form antibodies in the peritoneal cavity, but their antibody production is rather dependent on the splenic environment. Antibody forming cells (AFC-s) of B-1a origin can be also found in the bone marrow [89].

To address whether changes in B-1a lymphocyte homeostasis of Nkx2.3$^{-/-}$ mutant mice affect natural autoantibody production, total serum IgM, total serum IgG, PPS-specific IgM and phosphorylcholine (Pc) - specific IgM levels were measured at 1, 2 and 4 month of age in Nkx2.3$^{-/-}$ mutant and wild-type mice with ELISA technique.

According to our results, although the total serum IgM level was significantly lower in 1 month old mutant mice than in wild-type mice, the PPS- and Pc-specific IgM level decreased later, between 1 and 2 month of age, while during this period, the total serum IgM level did not show further substantial decrease. Although, the total, PPS- and Pc-specific IgM levels remained significantly lower in mutant mice at 4 month, no significant reduction of either fraction took place between 2 and 4 month (Figure 15.). Total serum IgG level did not differ considerably between the mutant and the wild-type mice at any time point (data not shown).

Thus, concerning PPS and Pc specificity, the natural antibody production of B-1a cells did not seem to completely depend on the intact splenic structure, but rather showed a correlation with the decrease in the ratio peritoneal CD5^{+} cells over time, with an enhanced decrease in young mice.

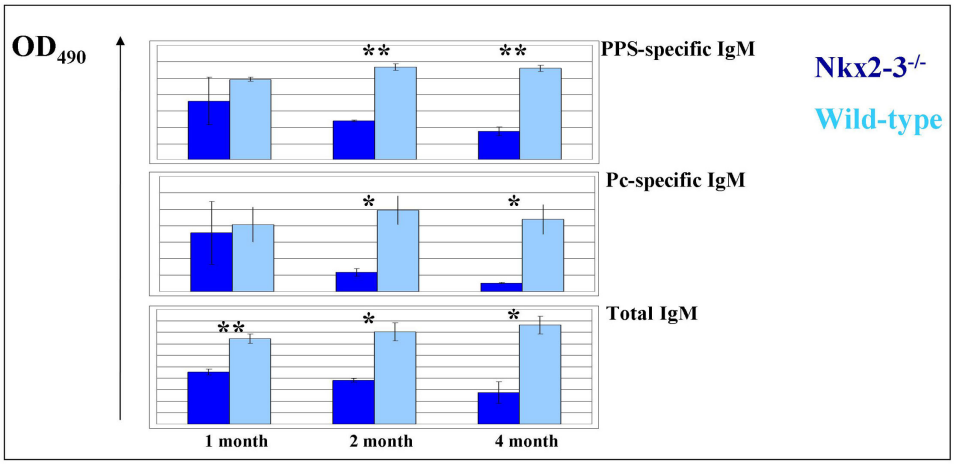

Figure 15. Changes in the serum level of PPS-, Pc-specific IgM and total IgM of Nkx2.3$^{-/-}$ mice at various ages. Histograms represent the serum level of PPS- and Pc-specific IgM (at 40x serum dilution) and total IgM (at 6250x serum dilution) of Nkx2.3$^{-/-}$ and control mice of various ages (n=4 per group) as the measure of OD490. Error bar = SEM, * p<0,05.

4.3.4 *B-1a cells are efficiently produced in Nkx2.3$^{-/-}$ mice*

Previous works addressing the dependence of B-1a homeostasis on the spleen has revealed that not only the postnatal maintenance, but also the fetal B-1a cell formation is dependent on the splenic environment [49].

In my experiments, although significantly reduced, a substantial fraction of peritoneal B-1a cells was present in 1 month old Nkx2.3$^{-/-}$ mutant mice, indicating an effective fetal B-1a cell formation in these mice. Therefore we aimed to examine to what extent a potentially decreased fetal CD5^{+} B-cell formation is responsible for this deficiency, or – alternatively – merely an abrogated postnatal maintenance results in the loss of this population.

In mice CD5^{+} B cells appear in the peritoneal cavity after the 8th postnatal day and acquire CD11b (Mac-1) expression during the first month [51]. To address the efficiency of fetal B-1a cell formation of Nkx2.3$^{-/-}$ mutant mice, peritoneal B-cell composition was examined 15 days postnatally, when – in wild-type mice – the majority of B lymphocytes are still CD5^{+} cells, and sufficient number of cells can be isolated from the peritoneal cavity for individual analysis, without the requirement for pooling samples. Therefore I extended the examination of peritoneal cell composition also including young postnatal mice.

I observed that within the peritoneal lymphocyte population, the majority of cells belonged to the CD5^{dim} B220^{dim} population (corresponding to CD5^{+} B cells) with an average

percentage of 38.2% and 44.7% in Nkx2.3$^{-/-}$ mutant and wild-type mice, respectively (Figure 16). The difference observed was not significant (p = 0,378), reflecting an efficient pre/perinatal CD5^{+} B lymphocyte production in mutant mice, indistinguishable from that in wt mice. Other cells either belonged to T cell (CD5^{+} B220^{-}) or B-2 cell (CD5^{-} B220^{+}) population, and a significant proportion of CD5^{-} B220^{-} was also present, probably representing a yet unidentified immature population.

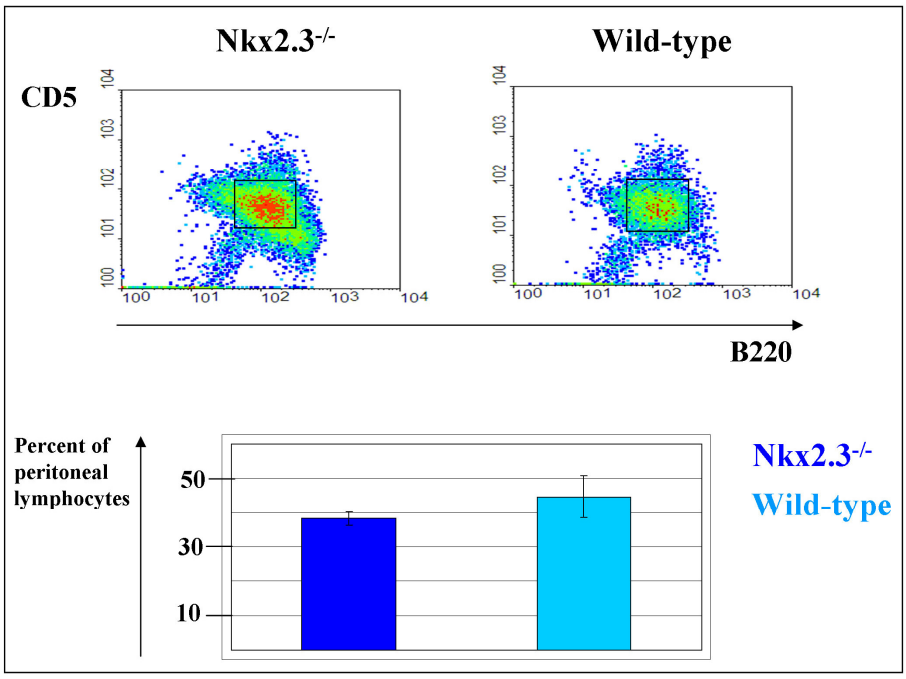

Figure 16. Efficient production of CD5^{+} B lymphocytes in neonatal Nkx2.3$^{-/-}$ mice. Peritoneal washout cells from 15 day old Nkx2.3$^{-/-}$ and BALB/c mice were dual-stained (B220 and CD5), and the ratio of CD5^{+} B lymphocytes within the peritoneal lymphocytes (as defined by FSC and SSC) was determined with flow-cytometry. n=3/group; Error bar = SEM; p=0,378.

4.3.5 *Diminished cell proliferation of CD5^{+} B cells may be responsible for altered homeostasis, and is the consequence of stromal alteration in Nkx2.3$^{-/-}$ mutant mice*

Based on my observations, after efficient fetal formation a progressive net loss of CD5^{+} B lymphocytes occurs postnatally in Nkx2.3$^{-/-}$ mutant mice. However, it is still unknown whether this process is a result of intrinsic defect of this B-lymphocyte subset, or results from the splenic stromal changes caused by the lack of Nkx2.3 HD transcription factor.

Furthermore, it is also elusive, to what extent reduced cell division or reduced cell survival is responsible for the net loss of this population over time**.**

To investigate this question, adoptive cell transfer experiment was performed. Total peritoneal washout cells from wild-type BALB/c mice were labeled *in vitro* with CFSE (as described in materials and methods), and intraperitoneally injected either to Nkx2.3$^{-/-}$ mutant or wild-type recipients. Two weeks after cell transfer, peritoneal cells were isolated from the recipients, and the ratio of total CFSE^{+} donor B-1a cells, and within this population, the already divided and not yet divided ratio has been determined (Figure 17).

I observed that in mutant mice, the ratio of CFSE-labeled donor CD5^{+} B lymphocytes within the total CD5^{+} B cell population was significantly lower than in wt recipients. The mean percentage ratio of these cells was 6,99% and 2,62 % in wild-type and Nkx2.3$^{-/-}$ mutant mice, respectively. As CFSE provides a stable fluorescent labeling of cells through covalent bound of the tracer compound to the intracellular proteins, it makes it suitable to compare the division rate of labeled donor cells after cell transfer. The CFSE content of labeled cells halves on each cell division. Consequently, cells that have undergone different number of divisions can be easily distinguished based on their fluorescent intensity. Accordingly, we assume that cells of maximal fluorescent intensity represent those that have not divided yet after the labeling. Using this distinction, we observed that on average 32,47% of donor CD5^{+} B lymphocytes have undergone at least one cell division in wild-type recipients, whereas in Nkx2.3$^{-/-}$ mutant recipients only a minor fraction (6,69 %) divided.

These results suggest that the progressive postnatal loss of CD5^{+} B lymphocytes in Nkx2.3$^{-/-}$ mutant mice is at least partially associated with diminished self-maintaining division of CD5^{+} lymphocytes, and is at least partially the consequence of the environmental alteration caused by the lack of Nkx2.3.

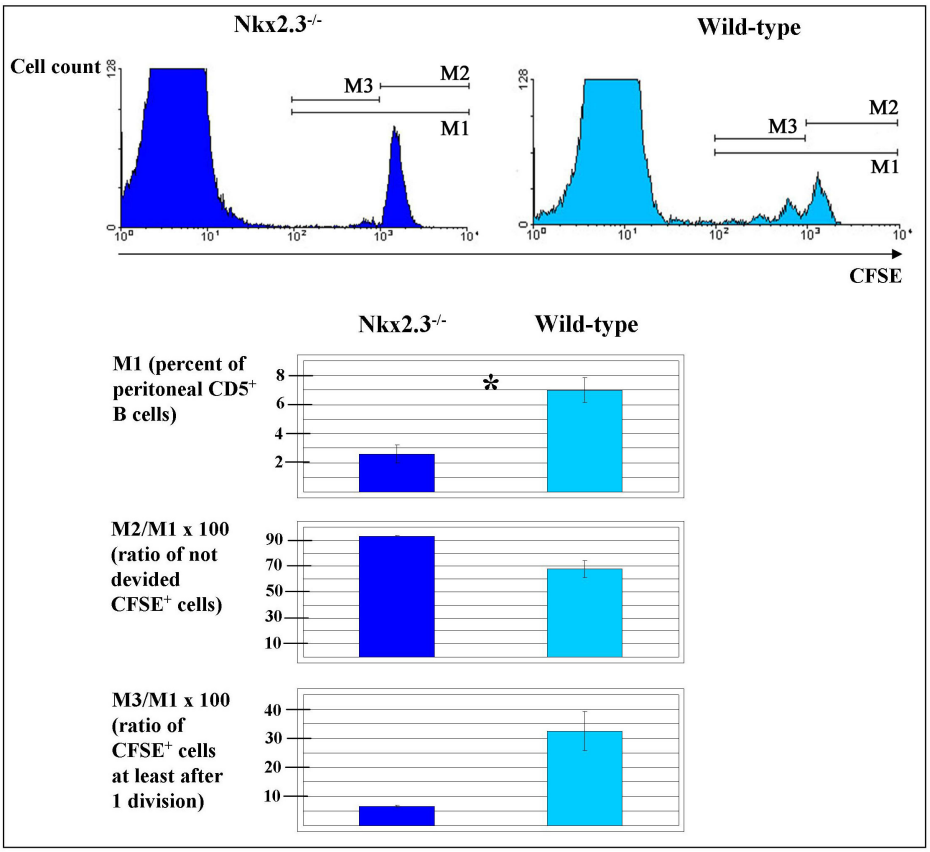

Figure 17. Altered self-maintaining division of CD5$^+$ B lymphocytes in Nkx2.3$^{-/-}$ mice. Total cells from BALB/c mice were *in vitro* labeled with CFSE and injected intraperitoneally (i.p.) either to Nkx2.3$^{-/-}$ or wild-type (BALB/c) recipients, as described in material and methods. Two weeks after cell transfer, peritoneal cells were isolated from the recipients, stained with B220, Mac-1 and CD5, and analyzed with flow cytometry. The ratio of total donor (CFSE$^+$) CD5$^+$ B lymphocytes were determined (M1 marked in the figure) followed by the determination of ratio of those cells that has not divided (M2 marked cells) as well as that has undergone at least one division (M3 marked population). n=3/group, Error bar = SEM, * p<0,05.

5 Short summary of the results

5.1. Endothelial reprogramming of the spleen in Nkx2.3$^{-/-}$ mutant mice results in the appearance of ectopic HEV-like vascular elements

Lymph node-like lymphoid cellular composition and lymph node-like endothelial transcription pattern of the spleen in Nkx2.3$^{-/-}$ mutant mice are coupled with the appearance of vascular segments that share several features with lymph node HEVs. These structures are lined by endothelial cells displaying the following characteristics:

- Co-express PNAd with HEC-GlcNAc6ST and CCL21, a modification enzyme required for functional PNAd formation, and an arrest chemokine indispensible for lymphocyte extravasation through HEV-s of the lymph nodes, respectively;
- Express PNAd in a lymphocyte-accessible manner on the luminal surface of the endothelium;
- Mediate lymphocyte extravasation in an L-selectin dependent manner.

All of these features are characteristics for the endothelial cells of HEV in pLN-s.

5.2. Establishing peritoneal B-1 cell exchange kinetics under steady state conditions as well as preferential redistribution after LPS stimulation through the introduction of a novel *in situ* fluorescent labeling technique

To investigate steady-state B-1 B cell distribution, a novel fluorescence-based labeling/tracing method was developed, and used to analyze serosal (peritoneal and pleural) replacement kinetics. This procedure serves as a reliable means for examining peritoneal lymphocyte homeostasis in wild-type as well as mutant animals over at least 4 weeks of duration.

Using this technique:

- we established the exact exchange kinetics of distinct peritoneal lymphocytes subsets (B-1, B-2 and T lymphocytes) on a so far unexamined time scale from 6 hours to 4 weeks post-labeling;
- we demonstrated that there is a mutual exchange between the peritoneal and pleural B-1 cell pool, as well as between the peritoneal B-cell pool and extraperitoneal B cells.

Thus changes in peritoneal B-1a lymphocyte population represents changes in the complete B-1a pool of the immune system, providing an easily accessible source for investigating B-1a homeostasis.

5.3. Progressive loss of $CD5^+$ B lymphocytes in $Nkx2.3^{-/-}$ mutant mice is associated with decreased self-maintaining division of these cells

Examining the peritoneal $CD5^+$ B cell ratio of $Nkx2.3^{-/-}$ mutant mice over time, we established that:

- Fetal production of this subset is not affected by the lack of Nkx2.3 transcription factor;
- B-1 B cells in KO mice have the same phenotype as wt B-1 cells;
- Decrease in the ratio of $CD5^+$ B cells progressively ensues postnatally, with an initial decrease in B-1c cells followed by the enhanced dissipation of B-1a cells;
- Decrease in the $CD5^+$ B cell ratio over time is accompanied by a decrease in the serum level of natural antibodies of different specificities.

With adoptive transfer of CFSE-labeled peritoneal cells we deciphered that altered homeostasis of $CD5^+$ B lymphocytes in $Nkx2.3^{-/-}$ mutant mice reflects functional changes associated with stromal abnormalities of these mice and the homeostatic defect is, at least partially, due to diminished self-maintaining division of these cells.

6 Discussion

Mechanism of structural development of lymphoid organs and its effect on the development and function of adaptive immune system are subjects of extensive studies; however, many details of the relationship between various lymphoid compartments are still unknown. In the first part of my studies, I examined the role of Nkx2.3 HD transcription factor in the vascular patterning of the spleen, a major lymphoid tissue with complex developmental traits. To address this question, we used Nkx2.3$^{-/-}$ mutant mouse model [25], [26], backcrossed to BALB/c background for 10 generations. Besides confirming earlier findings indicating that the lack of this transcription factor affects the vasculature of the red pulp, the marginal sinus as well as the white pulp, we demonstrated that the splenic vasculature undergoes a pLN-like reprogramming. As the most prominent result, ectopic HEV-like structures appear in the mutant spleen that are structurally and functionally equal to HEVs in pLN-s.

However, it is still unknown how the lack of Nkx2.3 brings about such a huge effect on the development of the spleen. It has been shown that Nkx2.3 is expressed in the spleen during embryonic life, when the red pulp sinusoid system of the spleen develops. Indeed, in Nkx2.3$^{-/-}$ mice the red pulp vasculature is affected to the most extent. Further changes in these mice, i.e. the lack of marginal sinus including MAdCAM-1 expressing sinus lining cells, disorganized white pulp stroma may be the indirect consequences of the lack of Nkx2.3, as these elements develop postnatally [15] [90] [91], when Nkx2.3 is not expressed anymore in the murine spleen. However, these changes may not be the exclusive consequence of the red pulp developmental defect; although on BALB/c background the red pulp is nearly completely absent in mutants ("*redless*" spleen), on other genetic background (C57BL/6) a reduced red pulp still develops, while the lack of Nkx2.3 results in the same changes concerning the marginal sinus and the white pulp. The only known target gene of Nkx2.3 is MAdCAM-1 [25], but its diminished expression can not explain the profound defect of MZ, MS and white pulp either, as in MAdCAM-1 deficient mice such aberrations were not found [92].

B-1a cells represent a unique, mainly fetal-derived, self-maintaining B-lymphocyte population which, through the formation of natural antibodies, may provide an innate-like

humoral defense against invading pathogens [33]. The adult B-cell repertoire is the result of the layered B-cell development consisting of B-1a cell and B-2 cell formation during fetal life and postnatally, respectively [40]. Presence of both lymphocyte populations proved to be non-redundant in establishing efficient humoral immune response against influenza virus [86]. In spite of their importance in immune response and their potential role in distinct human diseases [55] [59] [40], there are still many questions to be answered addressing the complete homeostasis of B-1a cells, including their production, maintenance, distribution and dependence on secondary lymphoid tissues, particularly the spleen [50] [49] [48].

One of our aims was to investigate the dependence of B-1a cells on the spleen over time, and for this we used Nkx2.3$^{-/-}$ mice. Although B-1a cells are also located in the spleen, pleural cavity, bone marrow (and B-1a derived IgA producing plasma cells in the gut [93] [94] [95]) around 40% of B-1a cells accumulate in the peritoneal cavity, where they form the major B-lymphocyte population. While analysing B-1a cell homeostasis, it is rather straightforward to isolate cells from this easily accessible place. However, the exact relationship of the peritoneal B-1a lymphocytes with B-1a lymphocytes of other niches is still not clear. Studies addressing the short-term peritoneal B-cell homeostasis and their distribution are typically based on the adoptive transfer of either *in vitro*-labeled or genotype-marked donor cells. As the homeostasis of peritoneal B-1a cells is regulated by a complex feedback mechanism resulting in a steady-state condition [40], induced leukocyte excess along with the *in vitro* manipulation of the donor cells, may influence the behaviour of both the donor and the recipient cells by disrupting equilibrium, thus affecting the results of experiments. Another approach to demonstrate the constant recirculation of B-1a cells is to establish parabiotic pairs between mice with different CD45 allotypes. However, in addition to the surgical intervention itself, it takes about 8 weeks until vascularization may connect the circulation of parabiotic partners, making the experiment relatively long. Furthermore, although mutual exchange of cells in the peritoneal and pleural cavities of the parabiotic animals was also reported, the origin of these cells could not be determined, i.e. for example whether B-1a lymphocytes in the peritoneal cavity of one partner originates from the peritoneal or pleural cavity of the partner [74]. Thus, our aim was to make use of the versatility of CFSE in an *in situ* intraperitoneal labeling procedure for examining peritoneal lymphocyte homeostasis and monitoring their distribution for longer period under preserved steady-state conditions, and apply this approach to Nkx2.3 deficient mice. Compared to other methods used so far for examining B-1a homeostasis, our technique requires less animal, is

suitable for a wide time scale (from 6 hours up until at least 4 weeks post labeling), requires less preparation, and examines B-1a homeostasis under more physiological conditions. Thus this method seems to be the most versatile means for addressing B-1a cell homeostasis under distinct circumstances. Our results acquired with this technique are summarized in Figure 18.

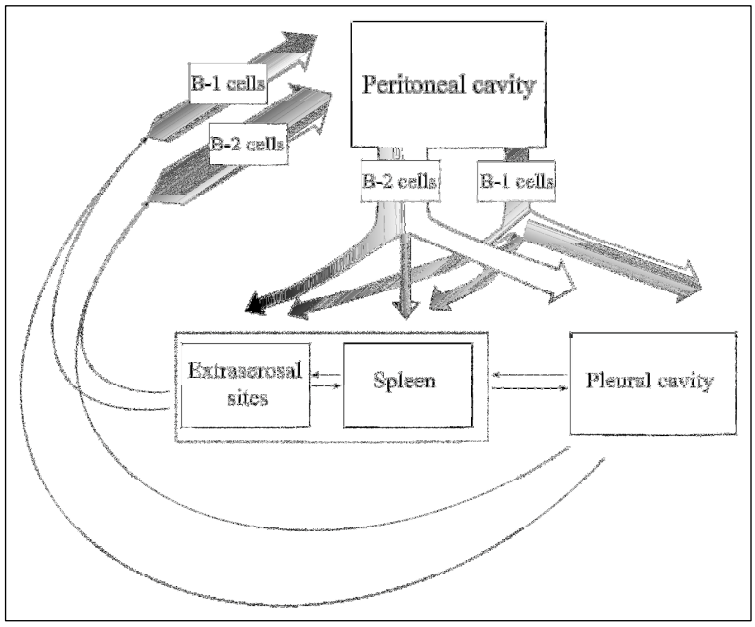

Figure 18. Overview of the exchange between the peritoneal and pleural B-cell compartments under steady-state conditions. Without LPS stimulation, B-2 cells are replaced faster in the peritoneal cavity (wider arrow) than B-1 cells, and the migration of both populations is preferentially directed toward the pleura, with lesser amount of cells homing to the spleen and extraserosal sites (narrower branches of both B-1 and B-2 arrows). This faster replacement of peritoneal B-2 cells may also be sustained by more active immigration/re-entry of B-2 cells from extraperitoneal sources. Upon LPS administration, the departure of B-cell subsets is differentially affected. For B-1 cells pleural, splenic and extraserosal accumulation are augmented (shading with widened arrowhead) in addition to proliferation induction (not depicted), while for B-2 cells, the pleural homing remains unaltered (empty branch of the arrow). The extent and kinetics of the exchange of both B-1 and B-2 cells among distinct extraperitoneal compartments are still unknown (dotted lines).

With the *in situ* intraperitoneal CFSE labeling technique we could prove the mutual exchange, as well as establish the exchange kinetics of B-1a cells and other peritoneal lymphocyte populations. Furthermore, we observed that after intraperitoneal LPS stimulation B-1a cells show a selective, enhanced pleural translocation in addition to cell division.

With this methodological background, next I investigated the effect of the lack of Nkx2.3 on the homeostasis of B-1a lymphocytes. In accordance with previous works indicating the importance of spleen in preserving B-1a cells [30], [48], [49], I found an age-dependent decrease of these cells. The continuous loss of these cells with the parallel loss of natural antibodies suggested that the red pulp-defective spleen in Nkx2.3 mice is unable to maintain this population. Furthermore, no differences were observed in the ratio of $CD5^+$ peritoneal B lymphocytes of 15 day old mutant and wild-type mice, implicating that the spleen of $Nkx2.3^{-/-}$ mutant mice initially is able to support the fetal production of B-1a cells. Alternatively, the spleen may not even be required for the fetal formation of this population, as there are no parallel data from Hox11 KO mice at such an early period.

Recently, the identification of B-1 cell progenitor within adult bone marrow seemed to resolve the debate concerning the origin of B-1a cells. Previously, two models have been established; the lineage model, and the induced-differentiation model [37], [40]. According to the latter, B-1 and B-2 lymphocytes originate from the same progenitor, and develop into the respective cell-type as the function of signal strength of BCR acquired during development. On the other hand, identification of a number of fetal tissues with B-1a cell formation potential (para-aortic splanchnopleura [PAS], aorto-gonad mesonephros [AGM], yolk sac, fetal liver), together with the later identification of a $CD19^+$ $B220^{low/neg}$ precursor [39], giving rise exclusively to B-1a and B-1b cells, favours the lineage hypothesis of B-1 cell origin. These precursors were also found in adult bone marrow, but not in the spleen. It is known that under steady state conditions, there is only a minimal B-1a production from the bone marrow, over time. However, under induced B-1a cell deficiency, adult bone marrow gives rise to a considerable proportion of B-1a cells with N'-nucleotide insertion in the BCR gene, a distinguishing feature of adult vs. fetal derived B-1a lymphocytes [55]. In accordance with all these data, it seems that the complete lack of spleen or the presence of spleen with altered structure (like in our Nkx2.3 KO mutants), the progressive loss of $CD5^+$ B lymphocytes partially results from the diminished self maintenance of fetal derived B-1a cells, which is coupled to the inability of adult bone marrow-derived B-1a cells to mature and make up for the loss of fetal B-1a cells. This may implicate further differences between fetal- adult B-1a cell formation with regards to their dependence on spleen. These results together with the recent identification of B-1a cell equivalents in humans [96] may help us understand the homeostasis of these cells in humans and their potential role in distinct disorders such as autoimmune diseases as well as hematologic malignancies.

7 References

1. **Mebius RE, Kraal G**. Structure and function of the spleen. *Nat. Rev. Immunol.* 2005; **5**:606–16.DOI: 10.1038/nri1669.

2. **Balogh P** ed. *Developmental Biology of Peripheral Lymphoid Organs*. Berlin, Heidelberg: Springer Berlin Heidelberg; 2011.DOI: 10.1007/978-3-642-14429-5.

3. **Chen Y, Pikkarainen T, Elomaa O, Soininen R, Kodama T, Kraal G, Tryggvason K**. Defective microarchitecture of the spleen marginal zone and impaired response to a thymus-independent type 2 antigen in mice lacking scavenger receptors MARCO and SR-A. *J. Immunol.* 2005; **175**:8173–80.

4. **Kang Y-S**. SIGN-R1, a novel C-type lectin expressed by marginal zone macrophages in spleen, mediates uptake of the polysaccharide dextran. *Int. Immunol.* 2003; **15**:177–186.DOI: 10.1093/intimm/dxg019.

5. **Stall AM, Wells SM, Lam KP**. B-1 cells: unique origins and functions. *Semin. Immunol.* 1996; **8**:45–59.DOI: 10.1006/smim.1996.0007.

6. **Choi YS, Dieter JA, Rothaeusler K, Luo Z, Baumgarth N**. B-1 cells in the bone marrow are a significant source of natural IgM. *Eur. J. Immunol.* 2012; **42**:120–9.DOI: 10.1002/eji.201141890.

7. **Arnon TI, Horton RM, Grigorova IL, Cyster JG**. Visualization of splenic marginal zone B-cell shuttling and follicular B-cell egress. *Nature*. 2013; **493**:684–8.DOI: 10.1038/nature11738.

8. **Ansel KM, Ngo VN, Hyman PL, Luther SA, Förster R, Sedgwick JD, Browning JL, *et al.*** A chemokine-driven positive feedback loop organizes lymphoid follicles. *Nature*. 2000; **406**:309–14.DOI: 10.1038/35018581.

9. **El Shikh MEM, El Sayed RM, Sukumar S, Szakal AK, Tew JG**. Activation of B cells by antigens on follicular dendritic cells. *Trends Immunol.* 2010; **31**:205–11.DOI: 10.1016/j.it.2010.03.002.

10. **Luther SA, Tang HL, Hyman PL, Farr AG, Cyster JG**. Coexpression of the chemokines ELC and SLC by T zone stromal cells and deletion of the ELC gene in the plt/plt mouse. *Proc. Natl. Acad. Sci. U. S. A.* 2000; **97**:12694–9.DOI: 10.1073/pnas.97.23.12694.

11. **Tellier J, Nutt SL**. The unique features of follicular T cell subsets. *Cell. Mol. Life Sci.* 2013; **70**:4771–84.DOI: 10.1007/s00018-013-1420-3.

12. **Bajénoff M, Glaichenhaus N, Germain RN**. Fibroblastic reticular cells guide T lymphocyte entry into and migration within the splenic T cell zone. *J. Immunol.* 2008; **181**:3947–54.

13. **Lokmic Z, Lämmermann T, Sixt M, Cardell S, Hallmann R, Sorokin L**. The extracellular matrix of the spleen as a potential organizer of immune cell compartments. *Semin. Immunol.* 2008; **20**:4–13.DOI: 10.1016/j.smim.2007.12.009.

14. **Balogh P**. Immunoarchitecture of distinct reticular fibroblastic domains in the white pulp of mouse spleen. *J. Histochem. Cytochem*. 2004; **Immunoarch**:1287–1298.

15. **Balázs M, Horváth G, Grama L, Balogh P**. Phenotypic identification and development of distinct microvascular compartments in the postnatal mouse spleen. *Cell. Immunol.* 2001; **212**:126–37.DOI: 10.1006/cimm.2001.1847.

16. **Bovári J, Czömpöly T, Olasz K, Arnold H-H, Balogh P**. Complex organizational defects of fibroblast architecture in the mouse spleen with Nkx2.3 homeodomain deficiency. *Pathol. Oncol. Res.* 2007; **13**:227–35.DOI: PAOR.2007.13.3.0227.

17. **Balogh P, Balázs M, Czömpöly T, Weih DS, Arnold H-H, Weih F**. Distinct roles of lymphotoxin-beta signaling and the homeodomain transcription factor Nkx2.3 in the ontogeny of endothelial compartments in spleen. *Cell Tissue Res.* 2007; **328**:473–86.DOI: 10.1007/s00441-007-0378-6.

18. **Brendolan A, Rosado MM, Carsetti R, Selleri L, Dear TN**. Development and function of the mammalian spleen. *Bioessays*. 2007; **29**:166–77.DOI: 10.1002/bies.20528.

19. **Hecksher-Sørensen J, Watson RP, Lettice LA, Serup P, Eley L, De Angelis C, Ahlgren U, *et al.*** The splanchnic mesodermal plate directs spleen and pancreatic laterality, and is regulated by Bapx1/Nkx3.2. *Development*. 2004; **131**:4665–75.DOI: 10.1242/dev.01364.

20. **Patterson KD, Drysdale TA, Krieg PA**. Embryonic origins of spleen asymmetry. *Development*. 2000; **127**:167–75.

21. **Kim B-M, Miletich I, Mao J, McMahon AP, Sharpe PA, Shivdasani RA**. Independent functions and mechanisms for homeobox gene Barx1 in patterning mouse stomach and spleen. *Development*. 2007; **134**:3603–13.DOI: 10.1242/dev.009308.

22. **Roberts CW, Shutter JR, Korsmeyer SJ**. Hox11 controls the genesis of the spleen. *Nature*. 1994; **368**:747–9.DOI: 10.1038/368747a0.

23. **Brendolan A, Ferretti E, Salsi V, Moses K, Quaggin S, Blasi F, Cleary ML, *et al.*** A Pbx1-dependent genetic and transcriptional network regulates spleen ontogeny. *Development*. 2005; **132**:3113–26.DOI: 10.1242/dev.01884.

24. **Koehler K, Franz T, Dear TN**. Hox11 is required to maintain normal Wt1 mRNA levels in the developing spleen. *Dev. Dyn.* 2000; **218**:201–6.DOI: 10.1002/(SICI)1097-0177(200005)218:1<201::AID-DVDY18>3.0.CO;2-R.

25. **Pabst O, Förster R, Lipp M, Engel H, Arnold HH**. NKX2.3 is required for MAdCAM-1 expression and homing of lymphocytes in spleen and mucosa-associated lymphoid tissue. *EMBO J.* 2000; **19**:2015–23.DOI: 10.1093/emboj/19.9.2015.

26. **Pabst O, Zweigerdt R, Arnold HH**. Targeted disruption of the homeobox transcription factor Nkx2-3 in mice results in postnatal lethality and abnormal development of small intestine and spleen. *Development*. 1999; **126**:2215–25.

27. **Wang CC, Biben C, Robb L, Nassir F, Barnett L, Davidson NO, Koentgen F, *et al.*** Homeodomain factor Nkx2-3 controls regional expression of leukocyte homing coreceptor MAdCAM-1 in specialized endothelial cells of the viscera. *Dev. Biol.* 2000; **224**:152–67.DOI: 10.1006/dbio.2000.9749.

28. **Gommerman JL, Browning JL**. Lymphotoxin/light, lymphoid microenvironments and autoimmune disease. *Nat. Rev. Immunol.* 2003; **3**:642–55.DOI: 10.1038/nri1151.

29. **Weih F, Caamaño J**. Regulation of secondary lymphoid organ development by the nuclear factor-kappaB signal transduction pathway. *Immunol. Rev.* 2003; **195**:91–105.

30. **Wang H, Feng J, Qi C, Morse HC**. An ENU-induced mutation in the lymphotoxin alpha gene impairs organogenesis of lymphoid tissues in C57BL/6 mice. *Biochem. Biophys. Res. Commun.* 2008; **370**:461–7.DOI: 10.1016/j.bbrc.2008.03.118.

31. **Medzhitov R, Janeway CA**. Innate immunity: the virtues of a nonclonal system of recognition. *Cell*. 1997; **91**:295–8.

32. **Hwang YY, McKenzie ANJ**. Innate lymphoid cells in immunity and disease. *Adv. Exp. Med. Biol.* 2013; **785**:9–26.DOI: 10.1007/978-1-4614-6217-0_2.

33. **Bendelac A, Bonneville M, Kearney JF**. Autoreactivity by design: innate B and T lymphocytes. *Nat. Rev. Immunol.* 2001; **1**:177–86.DOI: 10.1038/35105052.

34. **Herberman RB, Nunn ME, Holden HT, Lavrin DH**. Natural cytotoxic reactivity of mouse lymphoid cells against syngeneic and allogeneic tumors. II. Characterization of effector cells. *Int. J. Cancer*. 1975; **16**:230–9.

35. **Yokota Y, Mansouri A, Mori S, Sugawara S, Adachi S, Nishikawa S, Gruss P**. Development of peripheral lymphoid organs and natural killer cells depends on the helix-loop-helix inhibitor Id2. *Nature*. 1999; **397**:702–6.DOI: 10.1038/17812.

36. **Engel I, Murre C**. The function of E- and Id proteins in lymphocyte development. *Nat. Rev. Immunol.* 2001; **1**:193–9.DOI: 10.1038/35105060.

37. **Berland R, Wortis HH**. Origins and functions of B-1 cells with notes on the role of CD5. *Annu. Rev. Immunol.* 2002; **20**:253–300.DOI: 10.1146/annurev.immunol.20.100301.064833.

38. **Martin F, Kearney JF**. B1 cells: similarities and differences with other B cell subsets. *Curr. Opin. Immunol.* 2001; **13**:195–201.

39. **Dorshkind K, Montecino-Rodriguez E**. Fetal B-cell lymphopoiesis and the emergence of B-1-cell potential. *Nat. Rev. Immunol.* 2007; **7**:213–9.DOI: 10.1038/nri2019.

40. **Baumgarth N**. The double life of a B-1 cell: self-reactivity selects for protective effector functions. *Nat. Rev. Immunol.* 2011; **11**:34–46.DOI: 10.1038/nri2901.

41. **Haury M, Sundblad A, Grandien A, Barreau C, Coutinho A, Nobrega A**. The repertoire of serum IgM in normal mice is largely independent of external antigenic contact. *Eur. J. Immunol.* 1997; **27**:1557–63.DOI: 10.1002/eji.1830270635.

42. **Bos NA, Kimura H, Meeuwsen CG, De Visser H, Hazenberg MP, Wostmann BS, Pleasants JR, *et al.*** Serum immunoglobulin levels and naturally occurring antibodies against carbohydrate antigens in germ-free BALB/c mice fed chemically defined ultrafiltered diet. *Eur. J. Immunol.* 1989; **19**:2335–9.DOI: 10.1002/eji.1830191223.

43. **Hooijkaas H, Benner R, Pleasants JR, Wostmann BS**. Isotypes and specificities of immunoglobulins produced by germ-free mice fed chemically defined ultrafiltered "antigen-free" diet. *Eur. J. Immunol.* 1984; **14**:1127–30.DOI: 10.1002/eji.1830141212.

44. **Baumgarth N, Tung JW, Herzenberg L a**. Inherent specificities in natural antibodies: a key to immune defense against pathogen invasion. *Springer Semin. Immunopathol.* 2005; **26**:347–62.DOI: 10.1007/s00281-004-0182-2.

45. **Briles DE, Nahm M, Schroer K, Davie J, Baker P, Kearney J, Barletta R**. Antiphosphocholine antibodies found in normal mouse serum are protective against intravenous infection with type 3 streptococcus pneumoniae. *J. Exp. Med.* 1981; **153**:694–705.

46. **Kawahara T, Ohdan H, Zhao G, Yang Y-G, Sykes M**. Peritoneal cavity B cells are precursors of splenic IgM natural antibody-producing cells. *J. Immunol.* 2003; **171**:5406–14.

47. **Tumang JR, Francés R, Yeo SG, Rothstein TL**. Spontaneously Ig-secreting B-1 cells violate the accepted paradigm for expression of differentiation-associated transcription factors. *J. Immunol.* 2005; **174**:3173–7.

48. **Kretschmer K, Stopkowicz J, Scheffer S, Greten TF, Weiss S**. Maintenance of peritoneal B-1a lymphocytes in the absence of the spleen. *J. Immunol.* 2004; **173**:197–204.

49. **Wardemann H, Boehm T, Dear N, Carsetti R**. B-1a B cells that link the innate and adaptive immune responses are lacking in the absence of the spleen. *J. Exp. Med.* 2002; **195**:771–80.

50. **Szczepanek SM, McNamara JT, Secor ER, Natarajan P, Guernsey L a, Miller L a, Ballesteros E, *et al.*** Splenic morphological changes are accompanied by altered baseline immunity in a mouse model of sickle-cell disease. *Am. J. Pathol.* 2012; **181**:1725–34.DOI: 10.1016/j.ajpath.2012.07.034.

51. **Ghosn EEB, Yang Y, Tung J, Herzenberg L a, Herzenberg L a**. CD11b expression distinguishes sequential stages of peritoneal B-1 development. *Proc. Natl. Acad. Sci. U. S. A.* 2008; **105**:5195–200.DOI: 10.1073/pnas.0712350105.

52. **Krop I, de Fougerolles a R, Hardy RR, Allison M, Schlissel MS, Fearon DT**. Self-renewal of B-1 lymphocytes is dependent on CD19. *Eur. J. Immunol.* 1996; **26**:238–42.DOI: 10.1002/eji.1830260137.

53. **Deenen GJ, Kroese FG**. Kinetics of peritoneal B-1a cells (CD5 B cells) in young adult mice. *Eur. J. Immunol.* 1993; **23**:12–6.DOI: 10.1002/eji.1830230104.

54. **Hao Z, Rajewsky K**. Homeostasis of peripheral B cells in the absence of B cell influx from the bone marrow. *J. Exp. Med.* 2001; **194**:1151–64.

55. **Montecino-Rodriguez E, Dorshkind K**. B-1 B cell development in the fetus and adult. *Immunity*. 2012; **36**:13–21.DOI: 10.1016/j.immuni.2011.11.017.

56. **Kroese FG, Ammerlaan WA, Kantor AB**. Evidence that intestinal IgA plasma cells in mu, kappa transgenic mice are derived from B-1 (Ly-1 B) cells. *Int. Immunol.* 1993; **5**:1317–27.

57. **Kroese FG, Butcher EC, Stall a M, Lalor P a, Adams S, Herzenberg L a**. Many of the IgA producing plasma cells in murine gut are derived from self-replenishing precursors in the peritoneal cavity. *Int. Immunol.* 1989; **1**:75–84.

58. **Macpherson AJ, Gatto D, Sainsbury E, Harriman GR, Hengartner H, Zinkernagel RM**. A primitive T cell-independent mechanism of intestinal mucosal IgA responses to commensal bacteria. *Science*. 2000; **288**:2222–6.

59. **Duan B, Morel L**. Role of B-1a cells in autoimmunity. *Autoimmun. Rev.* 2006; **5**:403–8.DOI: 10.1016/j.autrev.2005.10.007.

60. **Hemmerich S, Bistrup A, Singer MS, Zante A Van, Lee JK, Tsay D, Peters M, *et al.*** Sulfation of L-Selectin Ligands by an HEV-Restricted Sulfotransferase Regulates Lymphocyte Homing to Lymph Nodes. *Immunity*. 2001; **15**:237–247.

61. **Nolte M**. Effects of fluorescent and nonfluorescent tracing methods on lymphocyte migration in vivo. *Cytom. A*. 2004; **61**:35–44.

62. **Imai Y**. Sulphation requirement for GlyCAM-1, an endothelial ligand for L-selectin. *Nature*. 1993; **361**:555–557.

63. **Baumheter S**. Binding of L-selectin to the vascular sialomucin CD34. *Science (80-.).* 1993; **262**:436–438.

64. **Berg E**. Lselectin– mediated lymphocyte rolling on MAdCAM-1. *Nature*. 1993; **366**:695–698.

65. **Umemoto E, Tanaka T, Kanda H, Jin S, Tohya K, Otani K, Matsutani T, *et al.*** Nepmucin, a novel HEV sialomucin, mediates L-selectin-dependent lymphocyte rolling and promotes lymphocyte adhesion under flow. *J. Exp. Med.* 2006; **203**:1603–14.DOI: 10.1084/jem.20052543.

66. **Sassetti C, Tangemann K, Singer MS, Kershaw DB, Rosen SD**. Identification of podocalyxin-like protein as a high endothelial venule ligand for L-selectin: parallels to CD34. *J. Exp. Med.* 1998; **187**:1965–75.

67. **Kanda H, Tanaka T, Matsumoto M, Umemoto E, Ebisuno Y, Kinoshita M, Noda M, *et al.*** Endomucin, a sialomucin expressed in high endothelial venules, supports L-selectin-mediated rolling. *Int. Immunol.* 2004; **16**:1265–74.DOI: 10.1093/intimm/dxh128.

68. **Rosen SD**. Ligands for L-selectin: homing, inflammation, and beyond. *Annu. Rev. Immunol.* 2004; **22**:129–56.DOI: 10.1146/annurev.immunol.21.090501.080131.

69. **Stanfel M**. Regulation of organ development by the NKX-homeodomain factors: an NKX code. *Cell. Mol. Biol. 51(Suppl. 51)*. 2005:OL785–OL799.

70. **Streeter PR, Rouse BT, Butcher EC**. Immunohistologic and functional characterization of a vascular addressin involved in lymphocyte homing into peripheral lymph nodes. *J. Cell Biol.* 1988; **107**:1853–62.

71. **Gallatin WM**. A cell-surface molecule involved in organ-specific homing of lymphocytes. *Nature*. 1983; **304**:30–34.

72. **Link A, Vogt TK, Favre S, Britschgi MR, Acha-Orbea H, Hinz B, Cyster JG, *et al.*** Fibroblastic reticular cells in lymph nodes regulate the homeostasis of naive T cells. *Nat. Immunol.* 2007; **8**:1255–65.DOI: 10.1038/ni1513.

73. **Gunn MD, Tangemann K, Tam C, Cyster JG, Rosen SD, Williams LT**. A chemokine expressed in lymphoid high endothelial venules promotes the adhesion and chemotaxis of naive T lymphocytes. *Proc. Natl. Acad. Sci. U. S. A.* 1998; **95**:258–63.

74. **Ansel KM, Harris RBS, Cyster JG**. CXCL13 is required for B1 cell homing, natural antibody production, and body cavity immunity. *Immunity*. 2002; **16**:67–76.

75. **Quah BJC, Warren HS, Parish CR**. Monitoring lymphocyte proliferation in vitro and in vivo with the intracellular fluorescent dye carboxyfluorescein diacetate succinimidyl ester. *Nat. Protoc.* 2007; **2**:2049–56.DOI: 10.1038/nprot.2007.296.

76. **Becker HM, Chen M, Hay JB, Cybulsky MI**. Tracking of leukocyte recruitment into tissues of mice by in situ labeling of blood cells with the fluorescent dye CFDA SE. *J. Immunol. Methods*. 2004; **286**:69–78.DOI: 10.1016/j.jim.2003.11.016.

77. **Genestier L, Taillardet M, Mondiere P, Gheit H, Bella C, Defrance T**. TLR agonists selectively promote terminal plasma cell differentiation of B cell subsets specialized in thymus-independent responses. *J. Immunol.* 2007; **178**:7779–86.

78. **Marcos MA, Huetz F, Pereira P, Andreu JL, Martinez-A C, Coutinho A**. Further evidence for coelomic-associated B lymphocytes. *Eur. J. Immunol.* 1989; **19**:2031–5.DOI: 10.1002/eji.1830191110.

79. **Kroese FG, Ammerlaan WA, Deenen GJ**. Location and function of B-cell lineages. *Ann. N. Y. Acad. Sci.* 1992; **651**:44–58.

80. **Hastings WD, Gurdak SM, Tumang JR, Rothstein TL**. CD5+/Mac-1- peritoneal B cells: a novel B cell subset that exhibits characteristics of B-1 cells. *Immunol. Lett.* 2006; **105**:90–6.DOI: 10.1016/j.imlet.2006.01.002.

81. **Allman D, Pillai S**. Peripheral B cell subsets. *Curr. Opin. Immunol.* 2008; **20**:149–57.DOI: 10.1016/j.coi.2008.03.014.

82. **Hippen KL, Tze LE, Behrens TW**. CD5 maintains tolerance in anergic B cells. *J. Exp. Med.* 2000; **191**:883–90.

83. **Baumgarth N**. B-cell immunophenotyping. *Methods Cell Biol.* 2004; **75**:643–62.

84. **Baumgarth N, Roederer M**. A practical approach to multicolor flow cytometry for immunophenotyping. *J. Immunol. Methods*. 2000; **243**:77–97.

85. **Wanga H**. NIH Public Access. *Biochem Biophys Res Commun*. 2008; **370**:461–467.DOI: 10.1016/j.bbrc.2008.03.118.An.

86. **Baumgarth N, Herman OC, Jager GC, Brown LE, Herzenberg L a, Chen J**. B-1 and B-2 cell-derived immunoglobulin M antibodies are nonredundant components of the protective response to influenza virus infection. *J. Exp. Med.* 2000; **192**:271–80.

87. **Savitsky D, Calame K**. B-1 B lymphocytes require Blimp-1 for immunoglobulin secretion. *J. Exp. Med.* 2006; **203**:2305–14.DOI: 10.1084/jem.20060411.

88. **Yang Y, Tung JW, Ghosn EEB, Herzenberg L a, Herzenberg L a**. Division and differentiation of natural antibody-producing cells in mouse spleen. *Proc. Natl. Acad. Sci. U. S. A.* 2007; **104**:4542–6.DOI: 10.1073/pnas.0700001104.

89. **Choi YS**. NIH Public Access. *Eur. J. Immunol*. 2012; **42**:120–129.DOI: 10.1002/eji.201141890.B-1.

90. **Chen Y, Pikkarainen T, Elomaa O, Kodama T, Kraal G, Soininen R, Tryggvason K**. This information is current as of July 10, 2013. *J. Immunol.* 2005; **175**:8173–8180.

91. **Balogh P, Aydar Y, Tew JG, Szakal a K**. Ontogeny of the follicular dendritic cell phenotype and function in the postnatal murine spleen. *Cell. Immunol.* 2001; **214**:45–53.DOI: 10.1006/cimm.2001.1874.

92. **Schippers A, Leuker C, Pabst O, Kochut A, Prochnow B, Gruber AD, Leung E, *et al.*** Mucosal addressin cell-adhesion molecule-1 controls plasma-cell migration and function in the small intestine of mice. *Gastroenterology*. 2009; **137**:924–33.DOI: 10.1053/j.gastro.2009.05.039.

93. **Kaminski D a, Stavnezer J**. Enhanced IgA class switching in marginal zone and B1 B cells relative to follicular/B2 B cells. *J. Immunol.* 2006; **177**:6025–9.

94. **Stoel M, Jiang H-Q, van Diemen CC, Bun JC a M, Dammers PM, Thurnheer MC, Kroese FGM, *et al.*** Restricted IgA repertoire in both B-1 and B-2 cell-derived gut plasmablasts. *J. Immunol.* 2005; **174**:1046–54.

95. **Ray A, Karmakar P, Biswas T**. Up-regulation of CD80-CD86 and IgA on mouse peritoneal B-1 cells by porin of Shigella dysenteriae is Toll-like receptors 2 and 6 dependent. *Mol. Immunol.* 2004; **41**:1167–75.DOI: 10.1016/j.molimm.2004.06.007.

96. **Griffin DO, Holodick NE, Rothstein TL**. Human B1 cells in umbilical cord and adult peripheral blood express the novel phenotype CD20+ CD27+ CD43+ CD70-. *J. Exp. Med.* 2011; **208**:67–80.DOI: 10.1084/jem.20101499.